PRISMA coupled to AGATA: characteristics, performance, possibilities and limitations

L.Corradi (LNL)

On behalf of the Prisma Collaboration

Agata Week
LNL, September 16-20, 2019

characteristics

PRISMA spectrometer – design characteristics

Angular acceptances $\Delta\theta \sim \pm 6^o$ $\Delta\phi \sim \pm 11^o$

Solid angle $\Delta\Omega \sim 80$ msr

Distance target-FPD 6.5 m

Energy acceptance ± 20%

Momentum acceptance ± 10%

Maximum Bρ = 1.2 Tm (ME/q^2 = 70 MeV amu)

Dispersion 4 cm/% Δp/p

Mass resolution 1/300 FWHM

Aberrations correction via software

MCP and MWPPAC x,y position resolutions 1 mm

MCP and MWPPAC timing resolutions ~ 350 ps

IC Energy resolution ~ 1%

Nuclear charge resolution ΔZ/Z ~ 1/60

PRISMA spectrometer – trajectory reconstruction

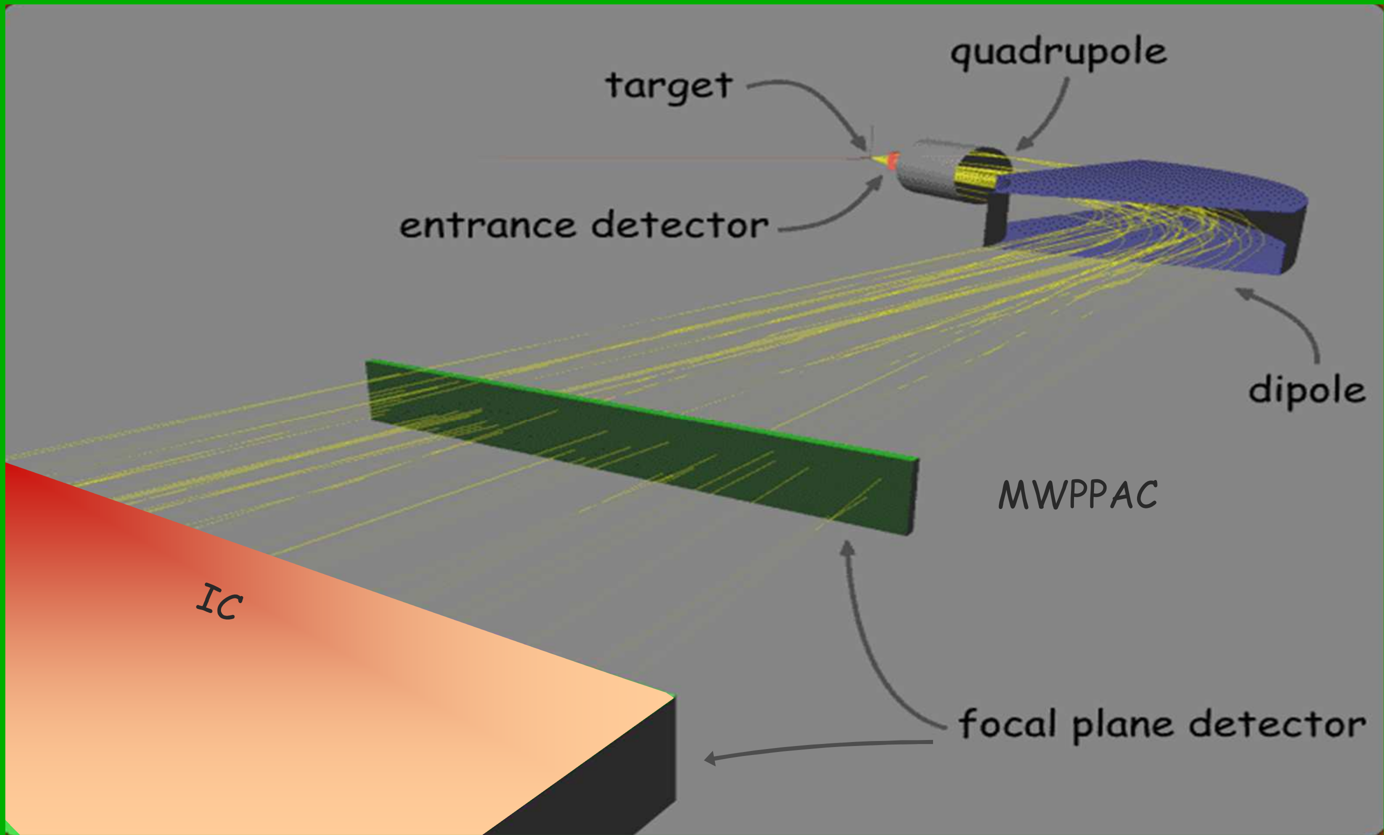

$$T = \frac{S(\theta, \phi)}{v}$$

$$B\rho = A \cdot \frac{v}{q} \propto X$$

$$q = \frac{2}{S(\theta, \phi)} \cdot \frac{E \cdot T}{B\rho(\theta, \phi)}$$

A physical event is composed by the parameters:

- position at the entrance x, y
- position at the focal plane X, Y
- time of flight TOF
- energy DE, E

PRISMA spectrometer – a complex detector system

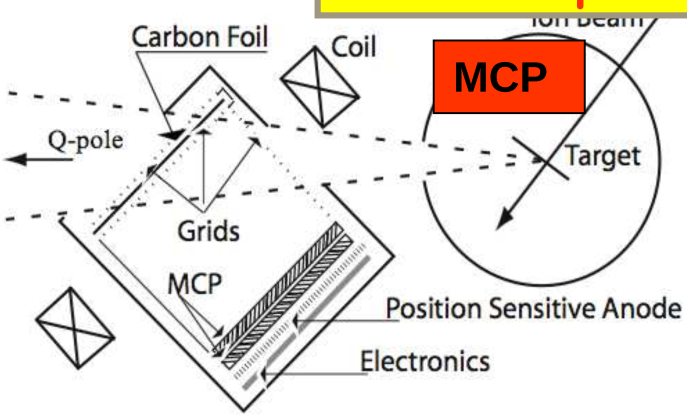

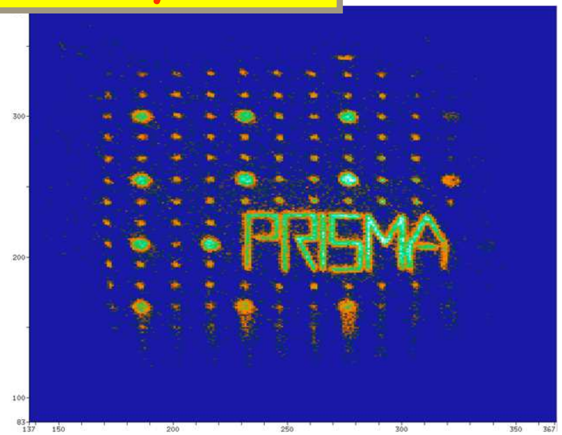

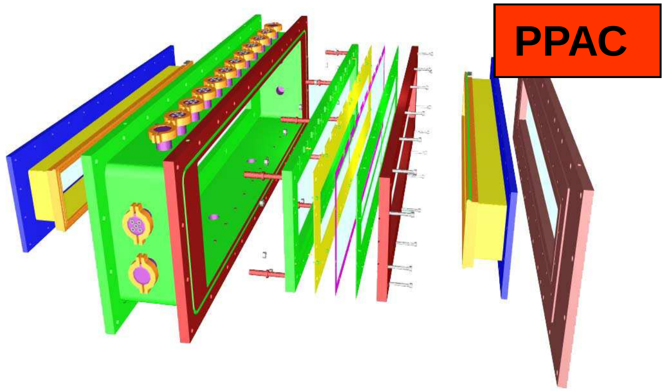

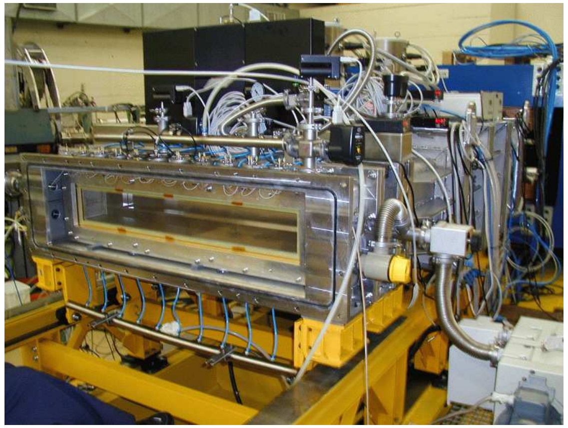

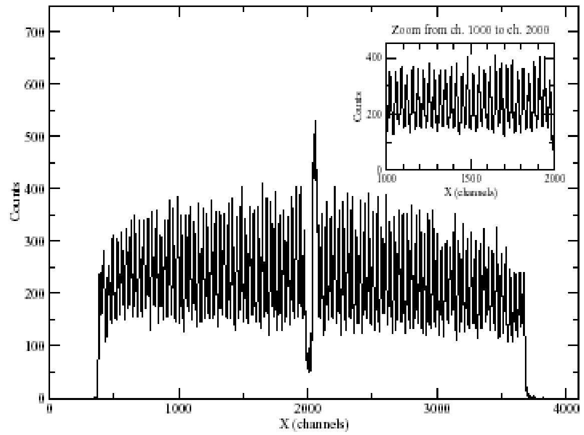

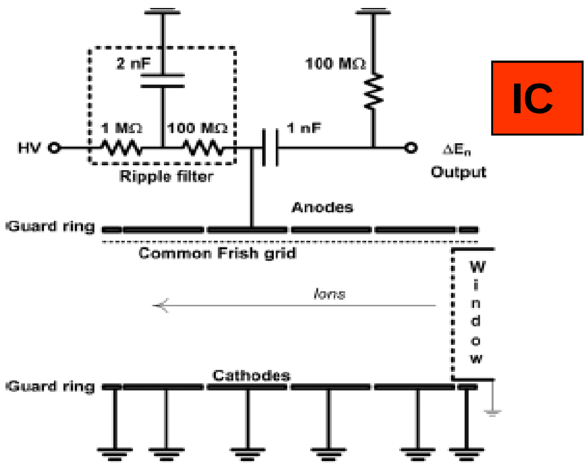

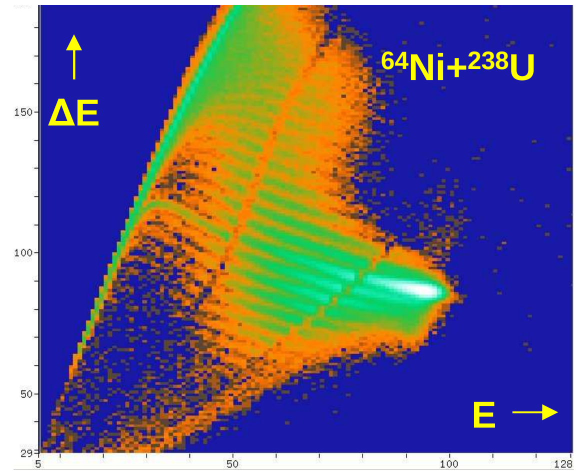

performance

DE – E matrix in $^{82}Se+^{238}U$ at E_{lab}=505 MeV, θ_{lab} = 64°

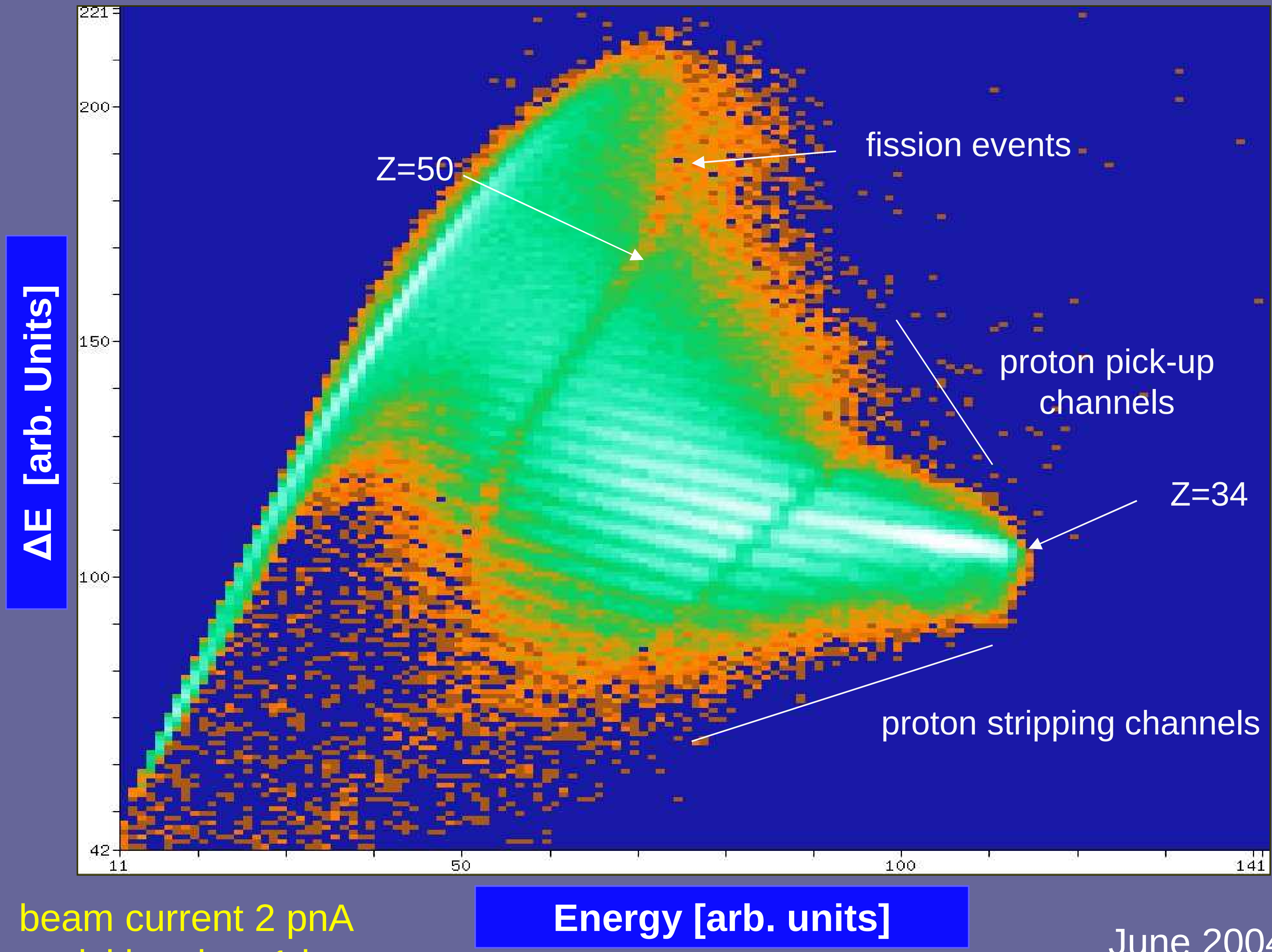

beam current 2 pnA
acquisition time 1 hour

June 2004

Beams accelerated for experiments with PRISMA

Grazing reactions as a tool to study n-rich nuclei

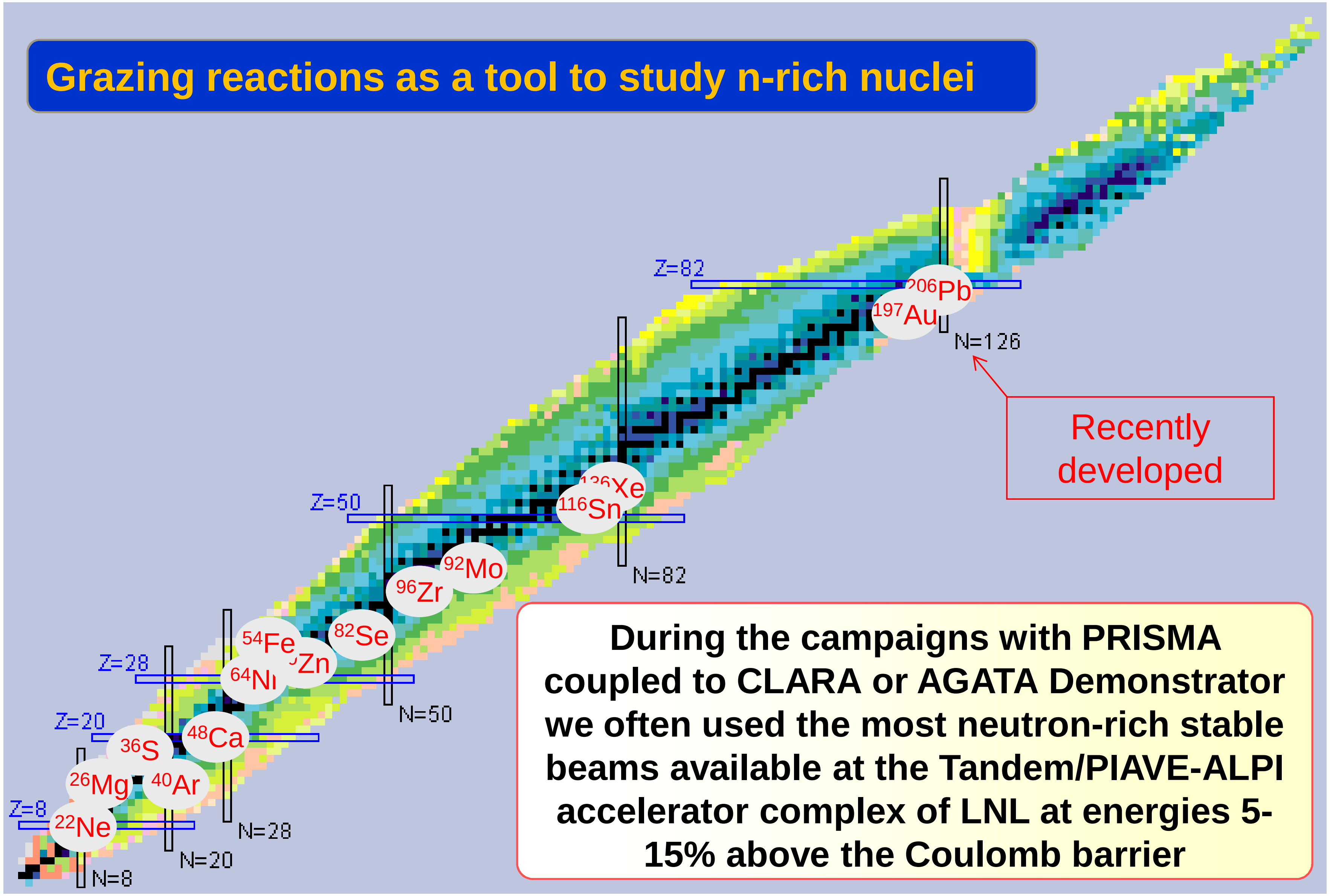

During the campaigns with PRISMA coupled to CLARA or AGATA Demonstrator we often used the most neutron-rich stable beams available at the Tandem/PIAVE-ALPI accelerator complex of LNL at energies 5-15% above the Coulomb barrier

Nuclear charge identification in the $^{206}Pb+^{118}Sn$ reaction

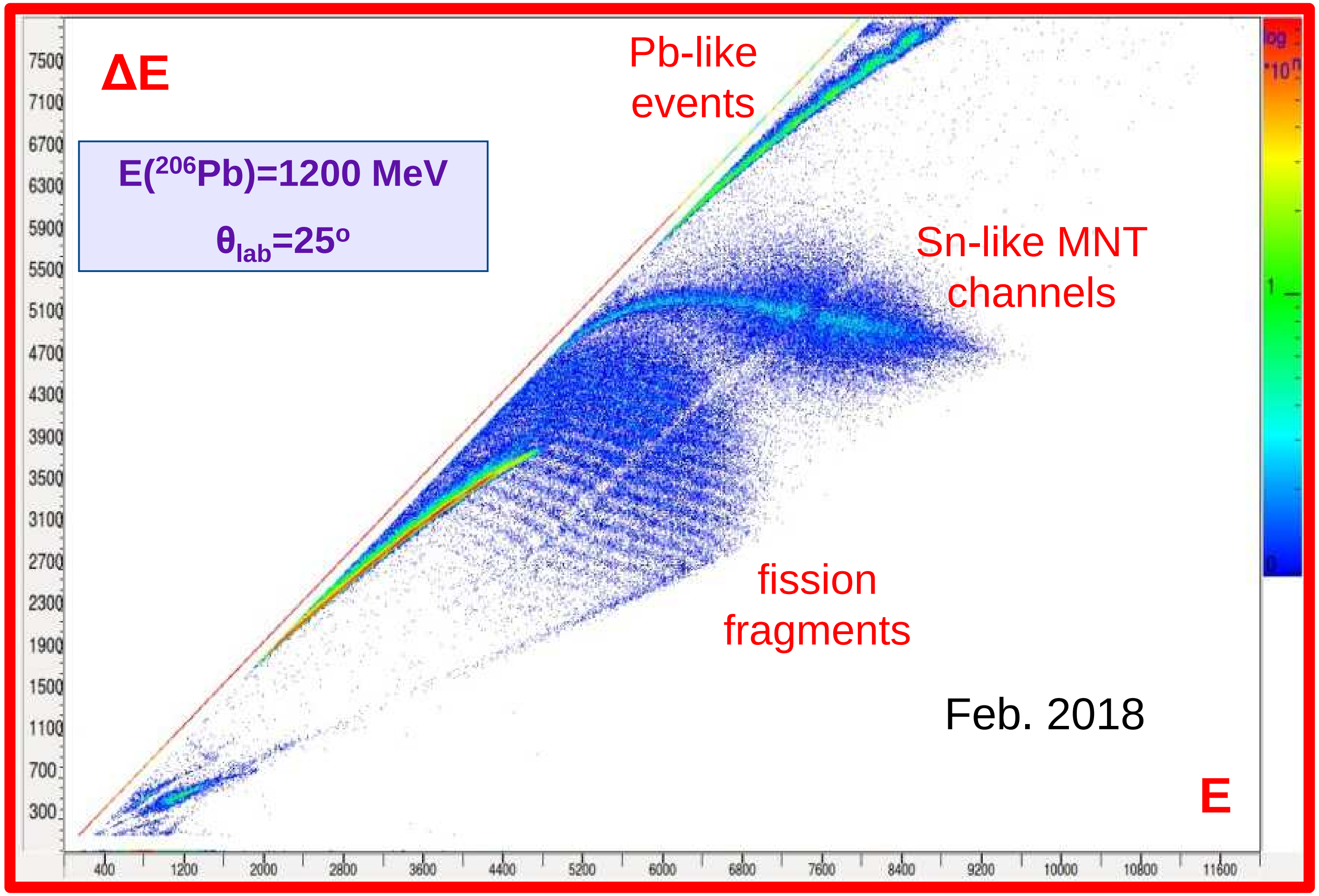

PRISMA was optimized for the detection of MNT channels but one can also observe a large yield for fission fragments, showing more clearly the obtained good Z-resolution

PRISMA spectrometer – trajectory reconstruction

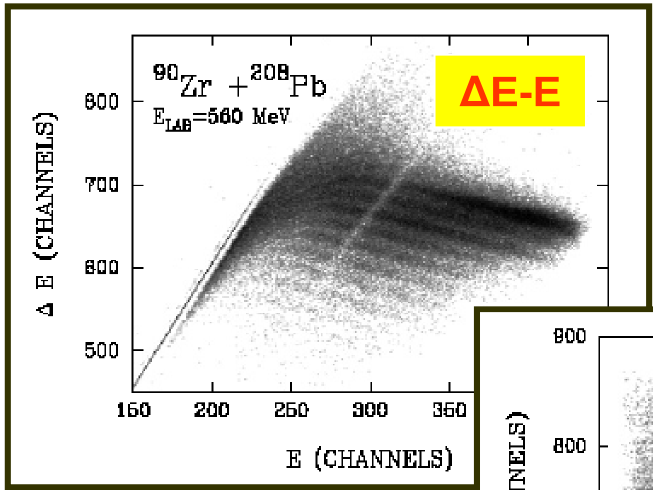

$$B\rho = A \cdot \frac{v}{q} \propto X$$

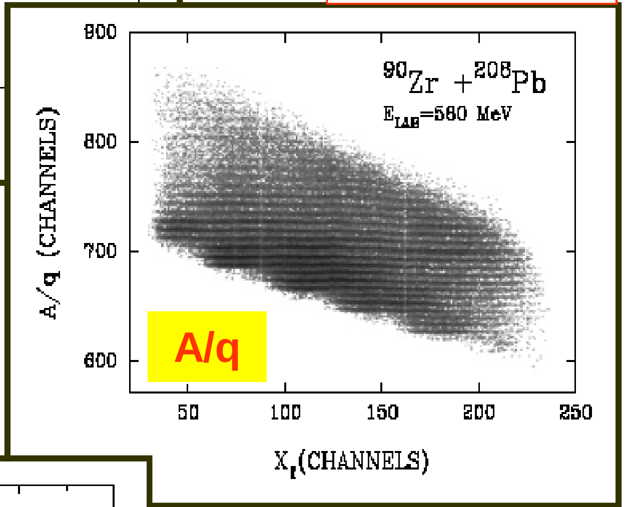

$$q = \frac{2}{S(\theta,\phi)} \cdot \frac{E \cdot T}{B\rho(\theta,\phi)}$$

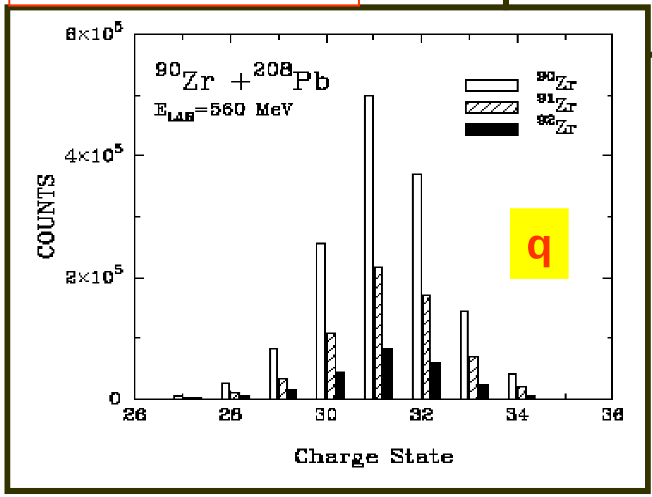

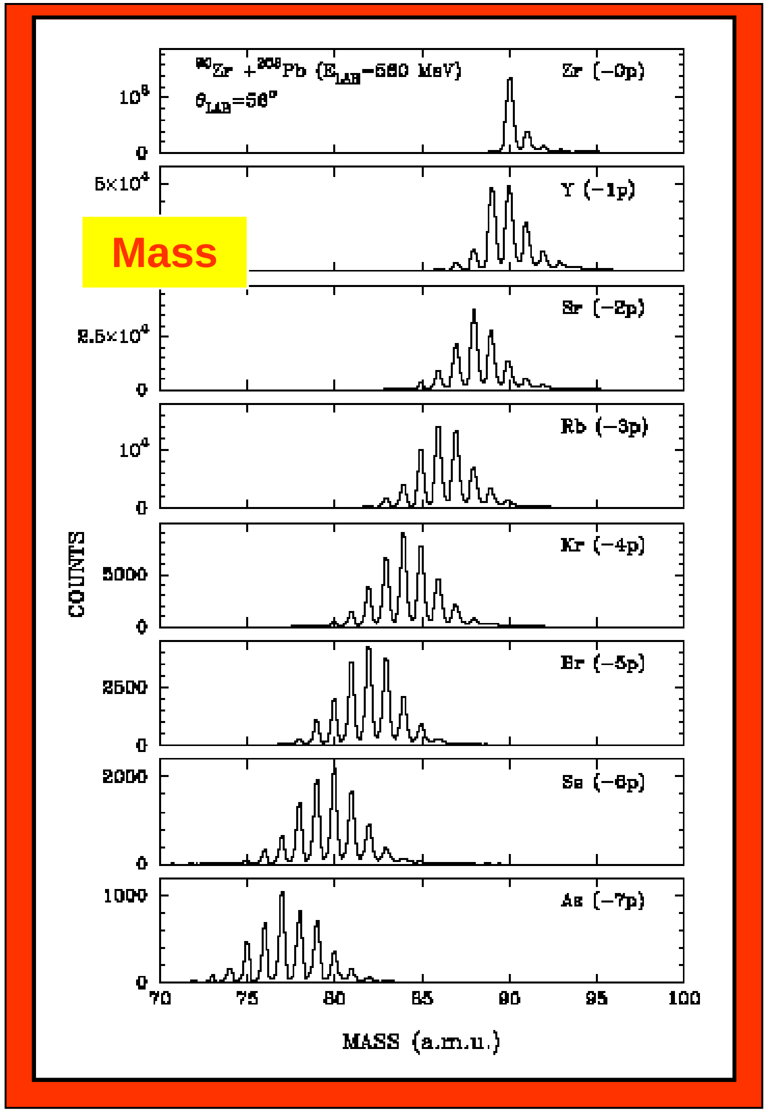

S.Szilner et al, PRC76(2007)024604

Mass resolution obtained after trajectory reconstruction

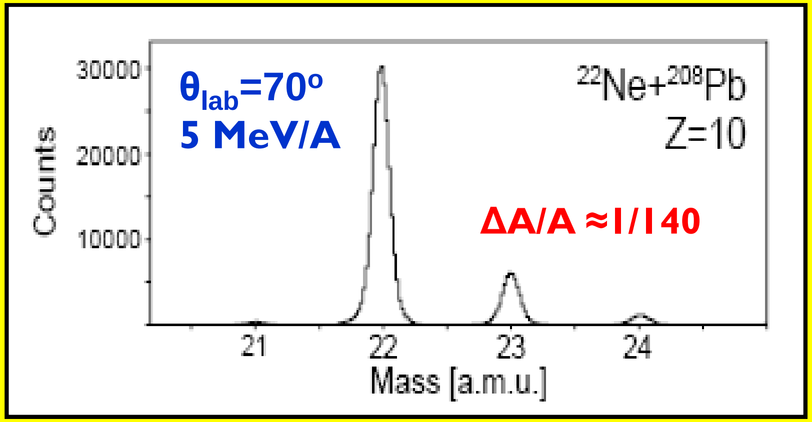

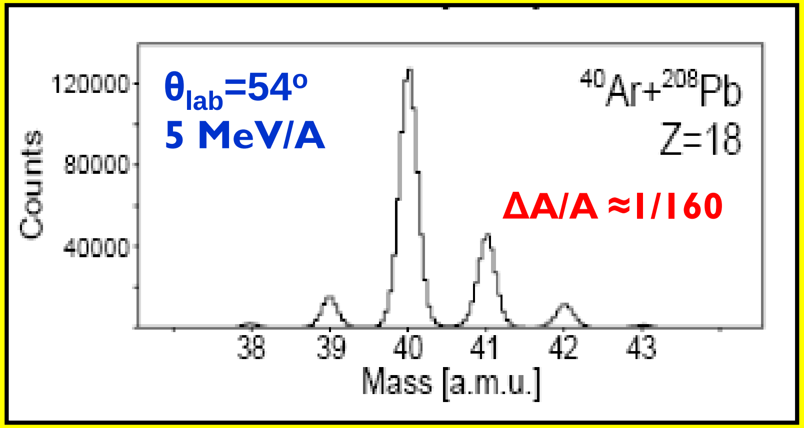

the obtained mass resolutions for the different ions are close to the values expected taking into account detector resolutions (positions and timing)

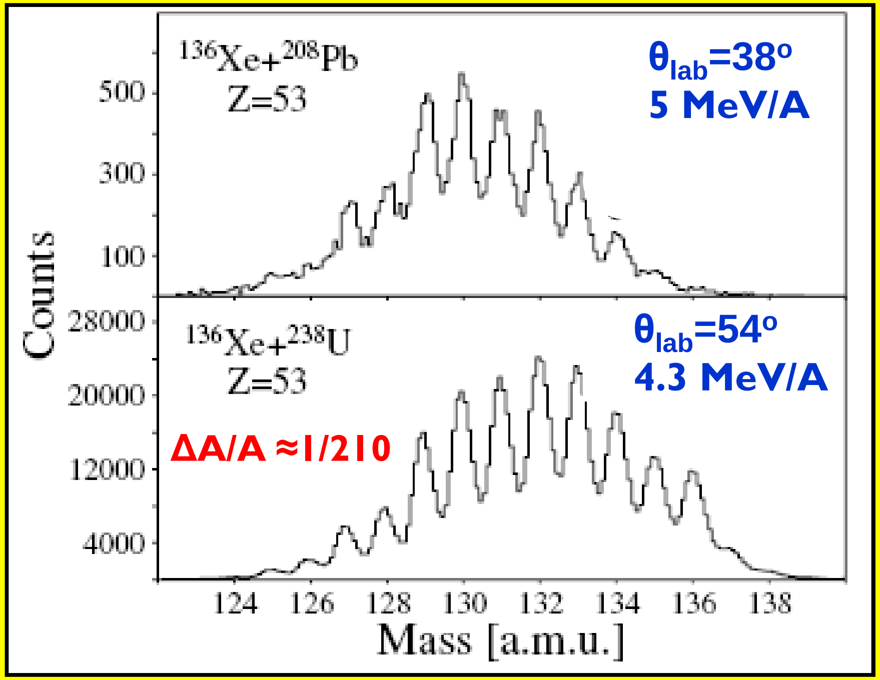

PRISMA spectrometer : MWPPAC detector at focal plane

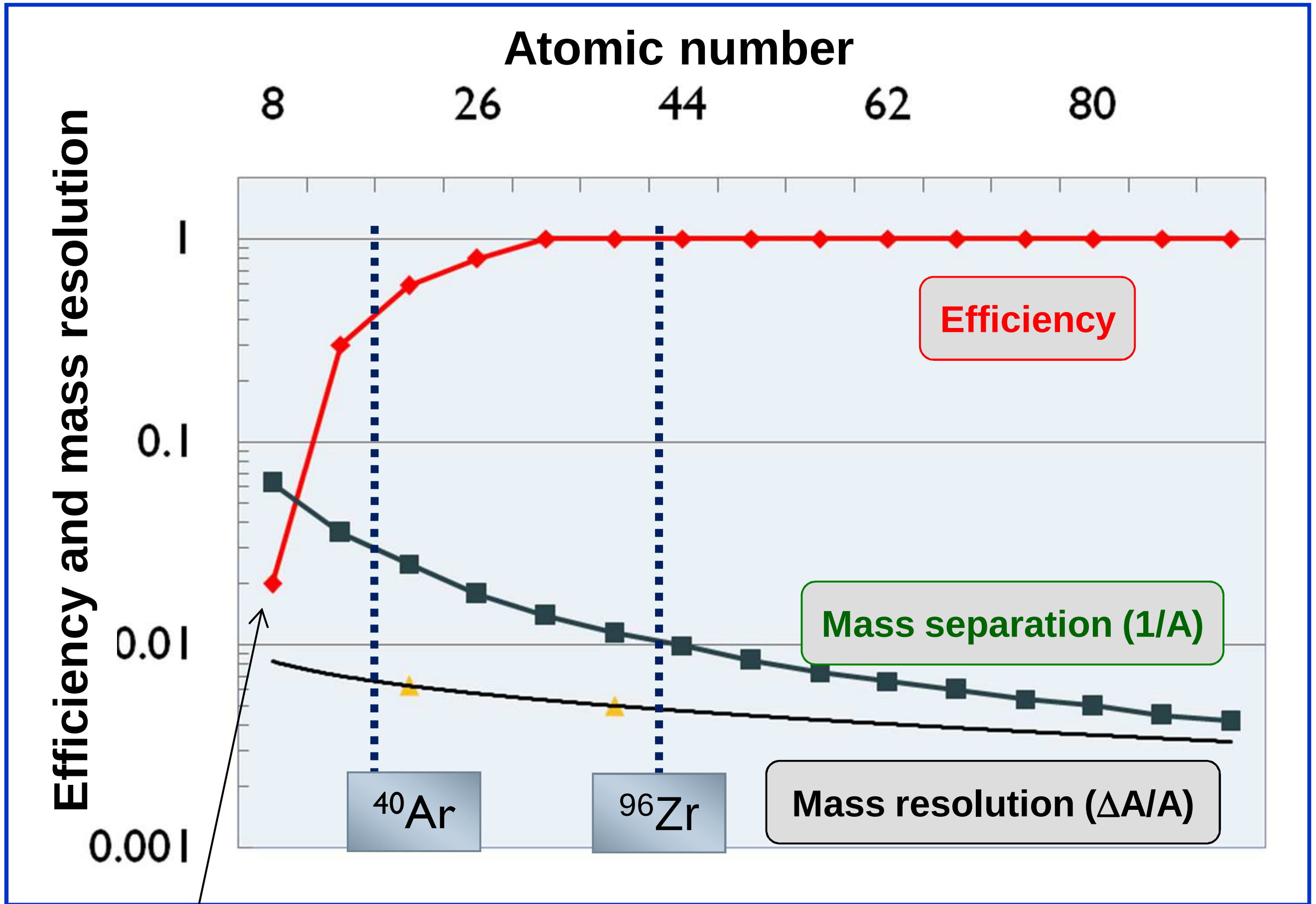

Attenuation of the X anode signals produced by the delay lines

cross sections

Multineutron and multiproton transfer channels near closed-shell nuclei

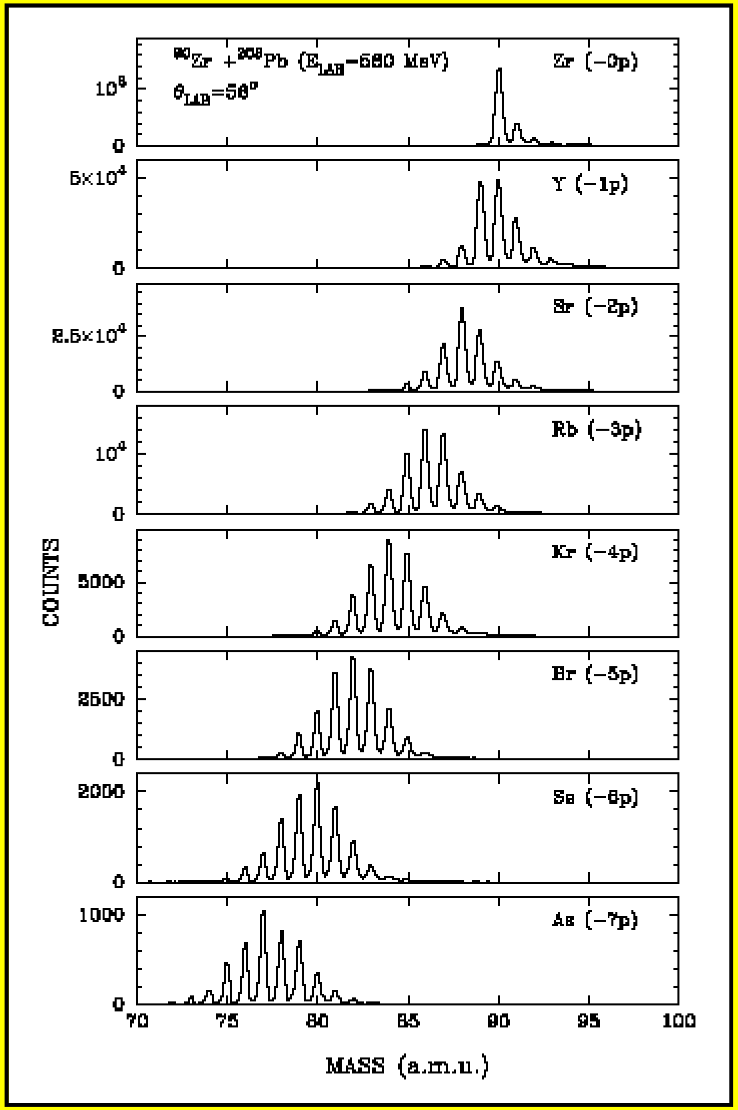

$^{90}Zr + ^{208}Pb$ E_{lab}=560 MeV

pure neutron pick-up channels

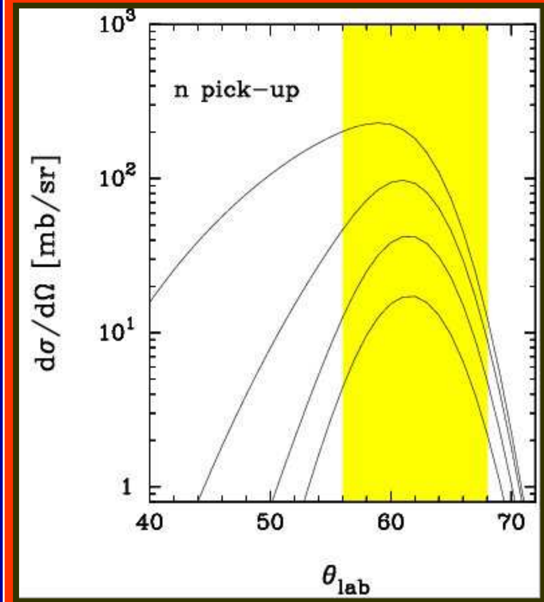

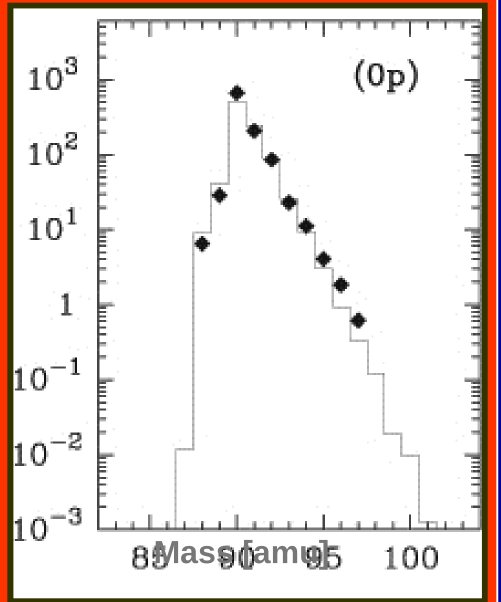

PRISMA spectrometer data

GRAZING code calculations

L.Corradi et al, J.Phys G36(2009)113101 (Topical Review)

Cross section sensitivity

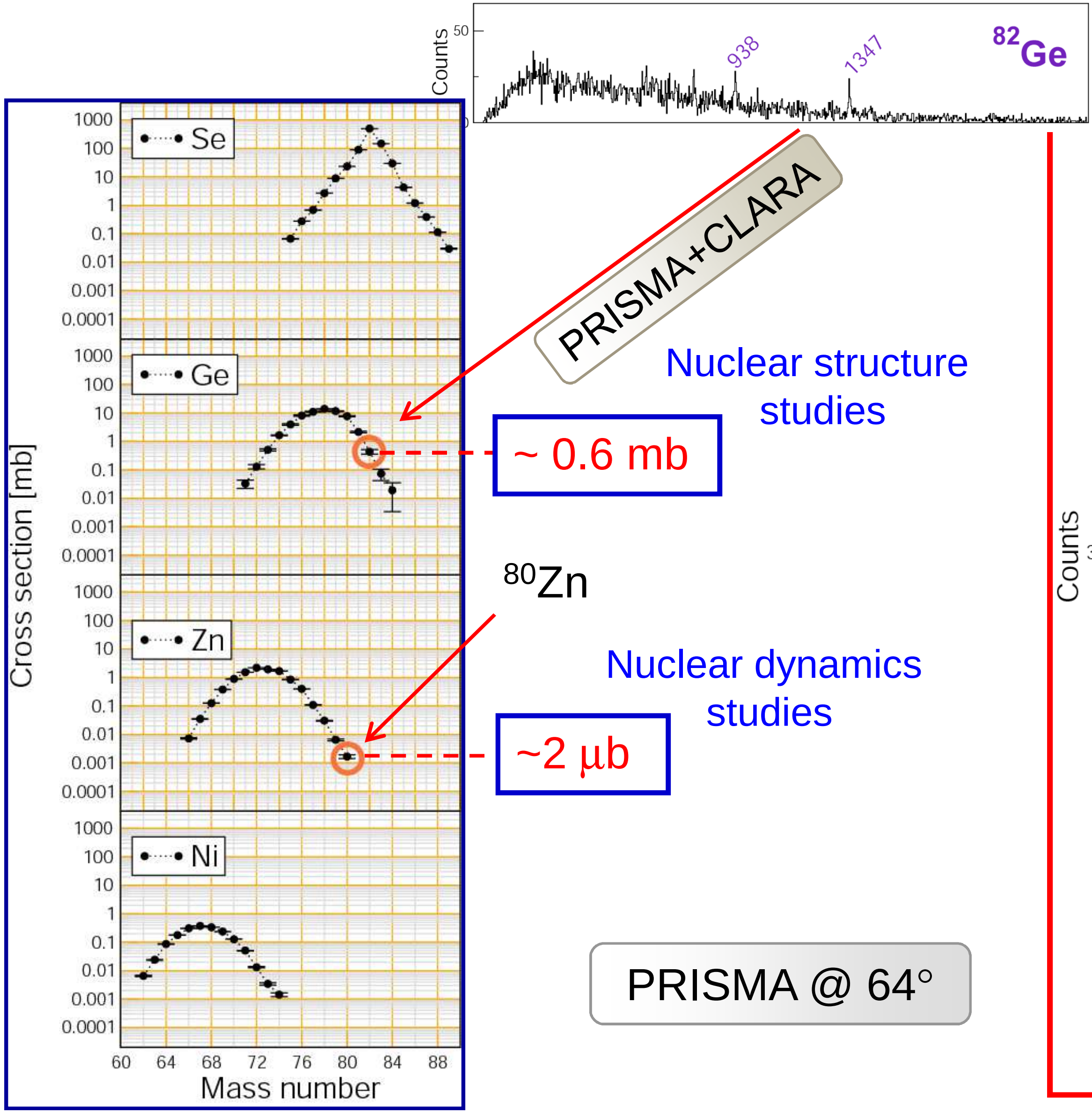

Nuclear structure studies

Nuclear dynamics studies

PRISMA @ 64°

$^{82}Se+^{238}U$ @ 505 MeV

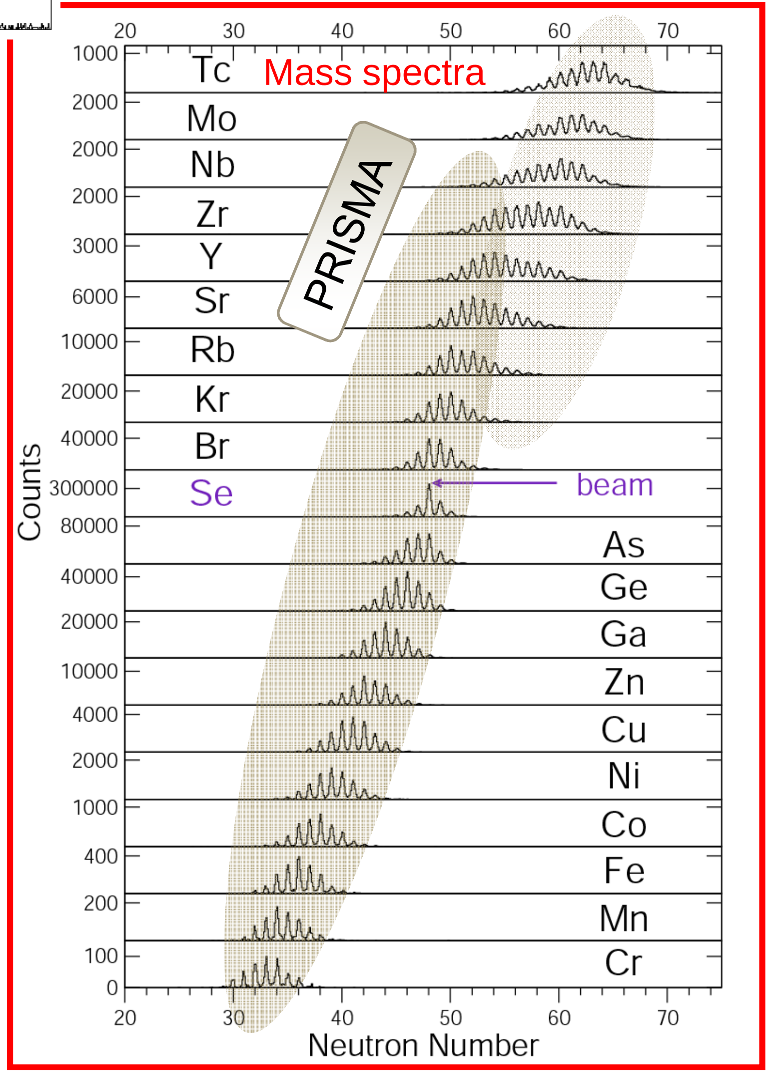

recent
developments

Detection of (light) target like ions in inverse kinematics with PRISMA

^{96}Zr ^{40}Ca L.Corradi et al, PRC84(2011)034603

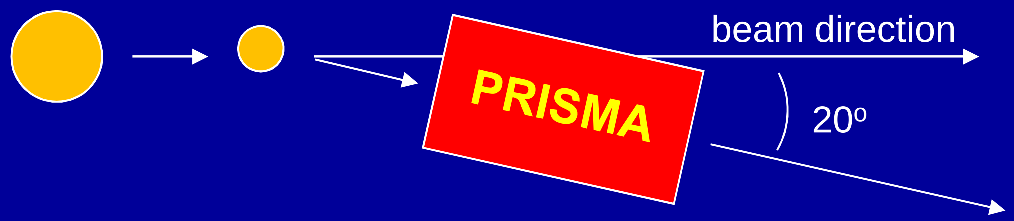

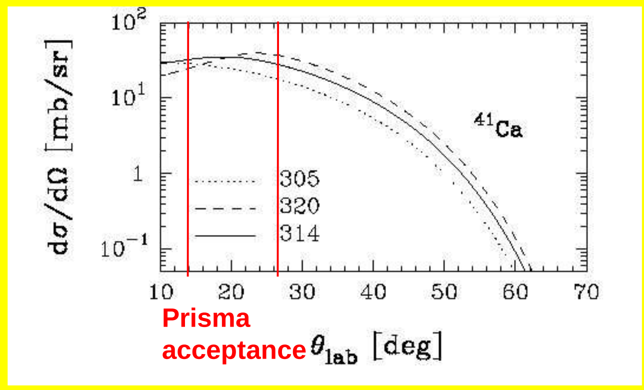

^{116}Sn ^{60}Ni D.Montanari et al, PRL113(2014)052501

^{92}Mo ^{54}Fe S.Szilner et al, in analysis phase

^{206}Pb ^{118}Sn L.Corradi et al, exp Feb. 2018

MNT channels have been measured down to 25 % below the Coulomb barrier

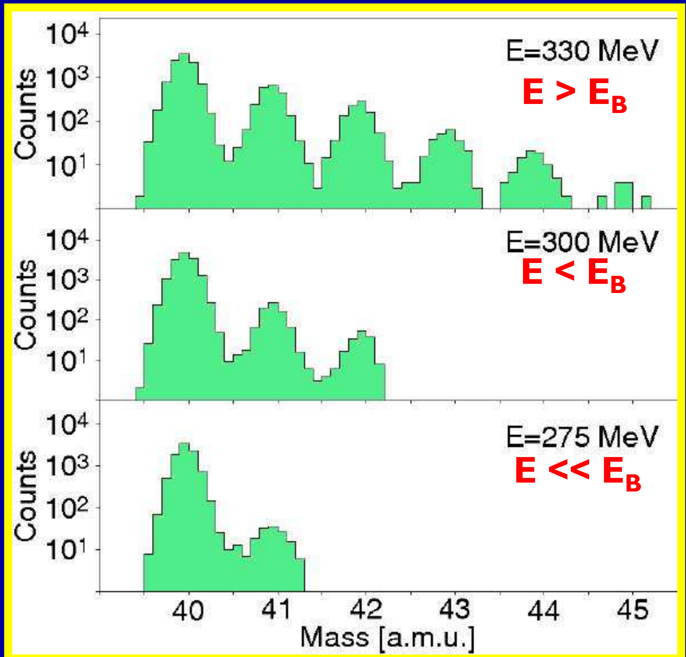

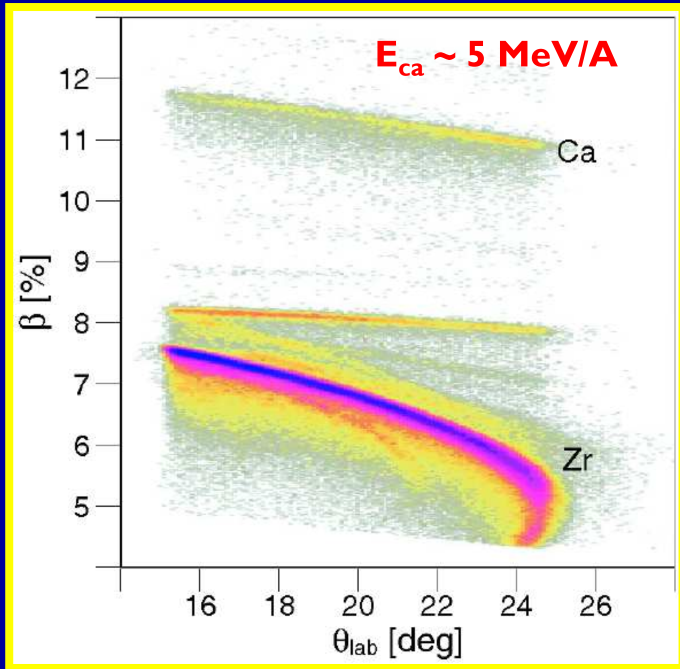

Transfer probabilities : comparison between exp and microscopic theory

$Q_{g.s.}$ for +2n + 5.5 MeV , far from Q_{opt} (~ 0 MeV)

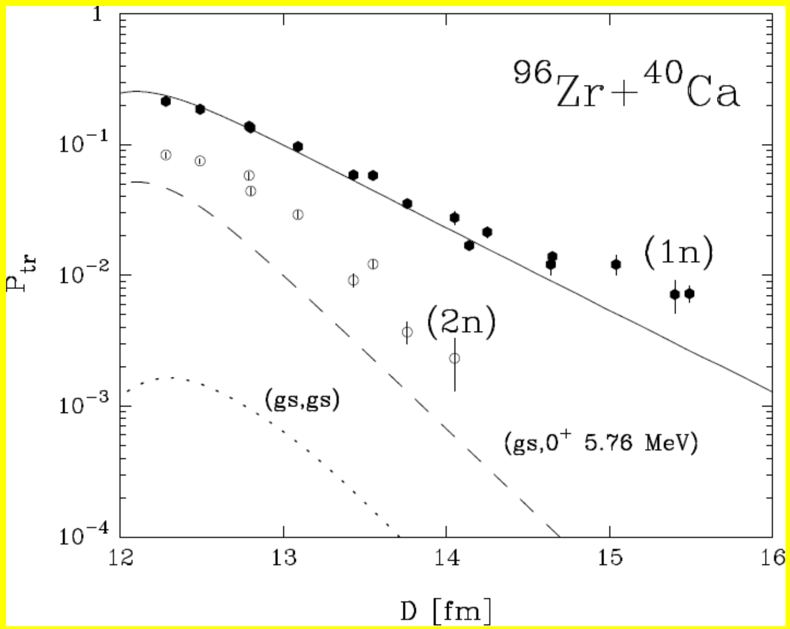

L.Corradi, S.Szilner, G.Pollarolo et al, PRC84(2011)034603

$Q_{g.s.}$ for +2n very close to Q_{opt} (~ 0 MeV)

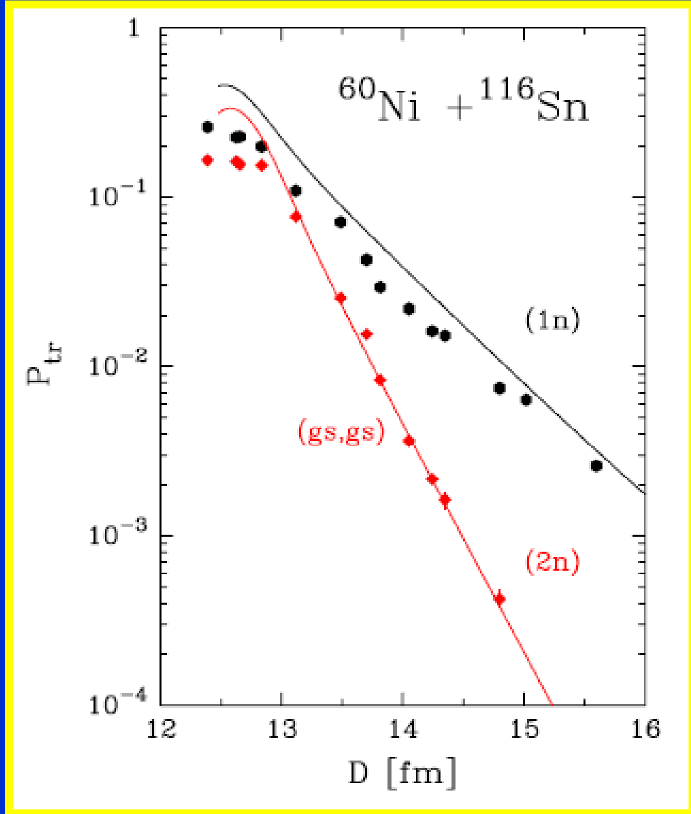

D.Montanari, L.Corradi, S.Szilner, G.Pollarolo et al, PRL113(2014)052501

Probing directly the population to the ground to ground states

from the gamma array one gets the strength to excited states ⟶ σ_{exc}

from the magnetic spectrometer one gets A,Z,Q (inclusive) ⟶ σ_{tot}

simplifying…

$$\sigma_{g.s.} = \sigma_{tot} - \sigma_{exc}$$

Pair neutron transfer probed via γ-particle coincidence in the $^{60}Ni+^{116}Sn$ system at E_{LAB}=245 MeV and $\theta_{LAB}=70^{\circ}$

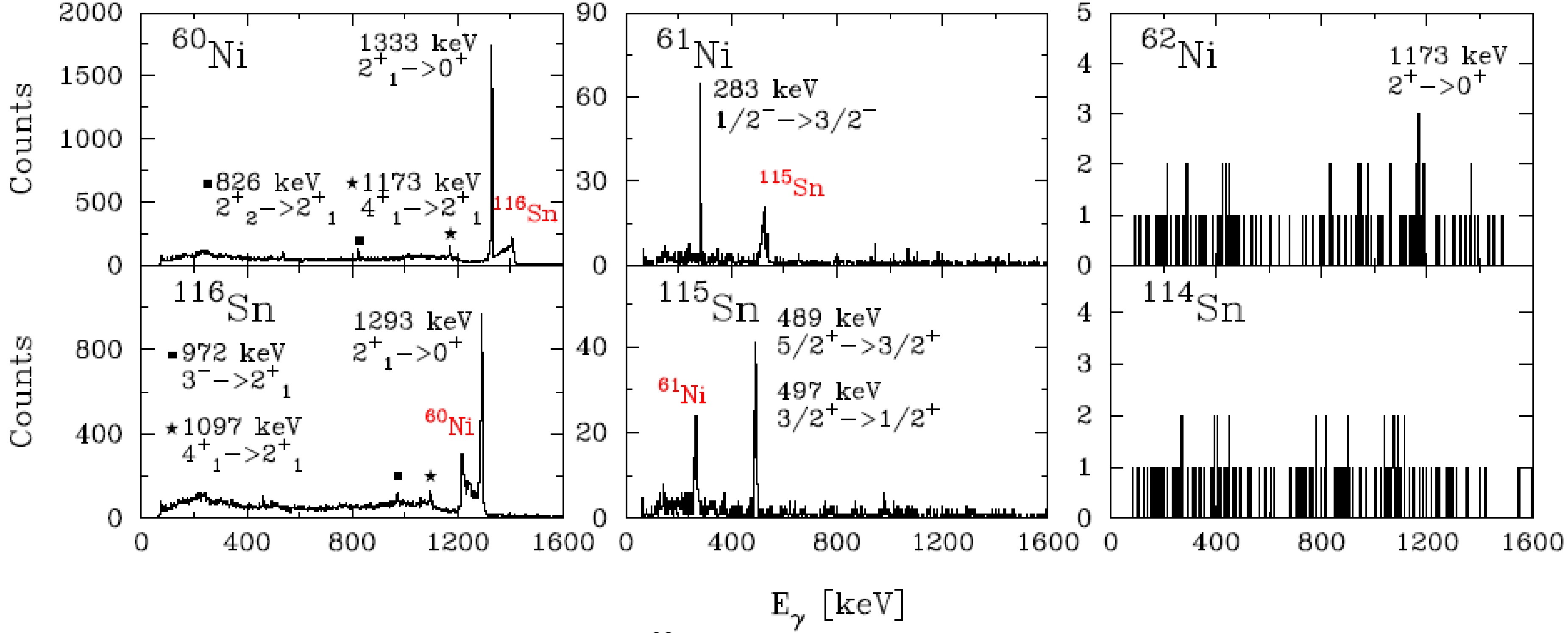

yields normalized to the 2^+ strength in ^{60}Ni

	Experiment	Theory
^{116}Sn(2^+)	0.792 ± 0.160	0.720
^{116}Sn(4^+_1)	0.042 ± 0.011	0.056
^{60}Ni(4^+_1)	0.060 ± 0.013	0.11
^{115}Sn($5/2^+$)	0.018 ± 0.003	0.037
^{61}Ni($1/2^-$)	0.014 ± 0.003	0.033
^{62}Ni(2^+)	< 0.00145	-

Experiment performed with PRISMA coupled to the AGATA DEMONSTRATOR

D.Montanari, L.Corradi, S.Szilner, G.Pollarolo et al, PRC93(2016)054623

Pair neutron transfer probed via γ-particle coincidence in the $^{60}Ni+^{116}Sn$ system at E_{LAB}=245 MeV and θ_{LAB}=70°

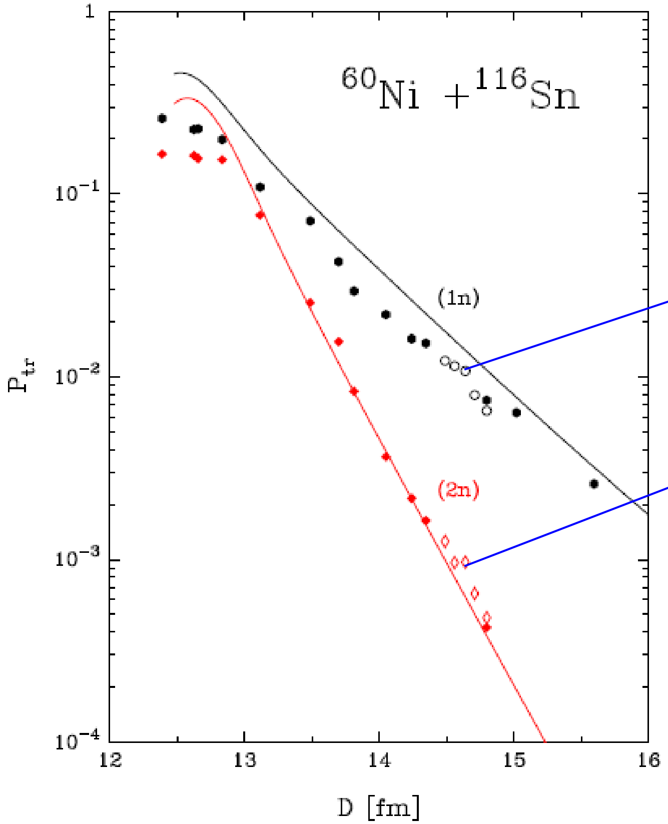

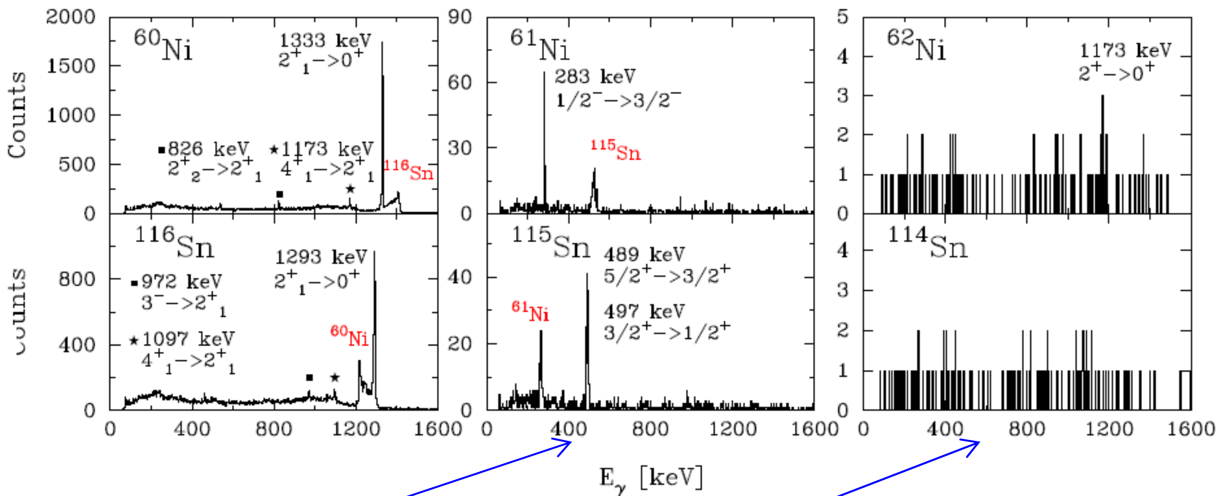

Experiment performed with PRISMA coupled to the AGATA DEMONSTRATOR

D.Montanari, L.Corradi, S.Szilner, G.Pollarolo et al, PRC93(2016)054623

The ^{197}Au+^{130}Te experiment with the PRISMA spectrometer

^{197}Au + ^{130}Te @ E_{lab}= 1.07 GeV inverse kinematics

PRISMA spectrometer used in high resolution kinematic coincidence with a second time-of-flight system (NOSE)

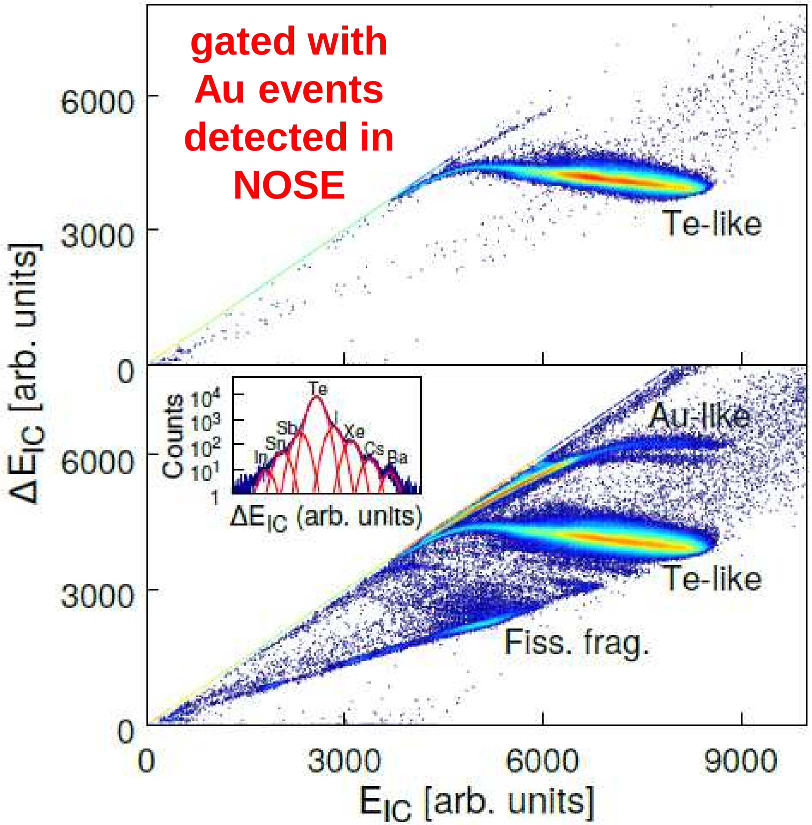

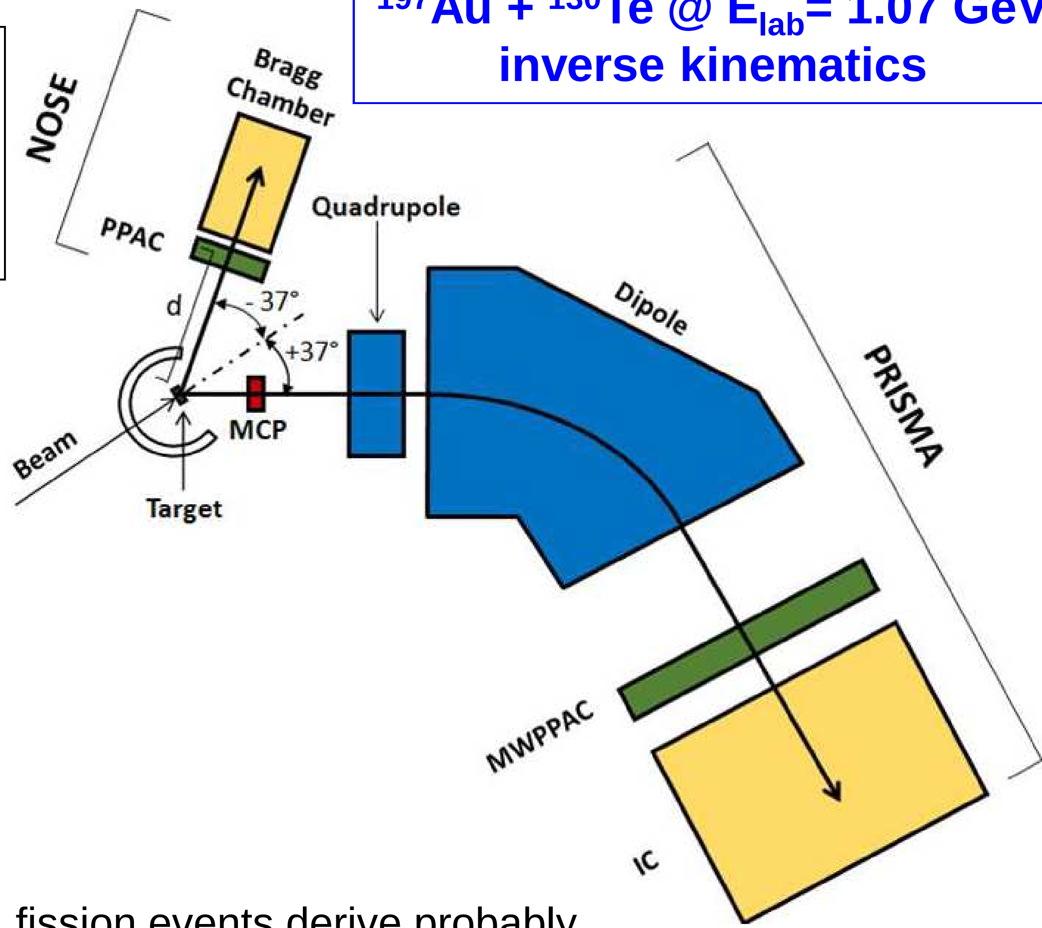

fission events derive probably from transfer induced fission or quasi fission

F.Galtarossa et al., Phys. Rev. C97(2018)054606

The $^{197}Au+^{130}Te$ experiment with the PRISMA spectrometer

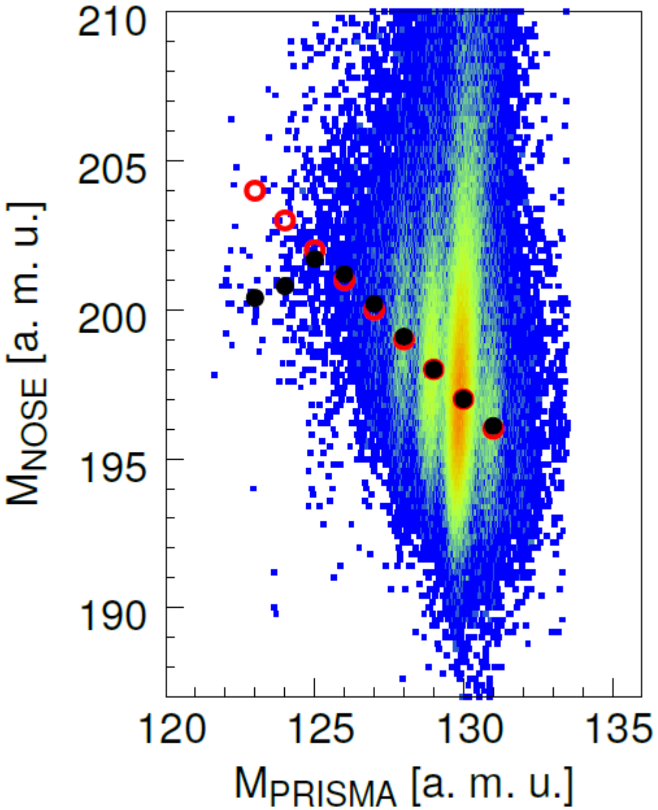

$^{197}Au + ^{130}Te$ @ E_{lab}= 1.07 GeV
inverse kinematics

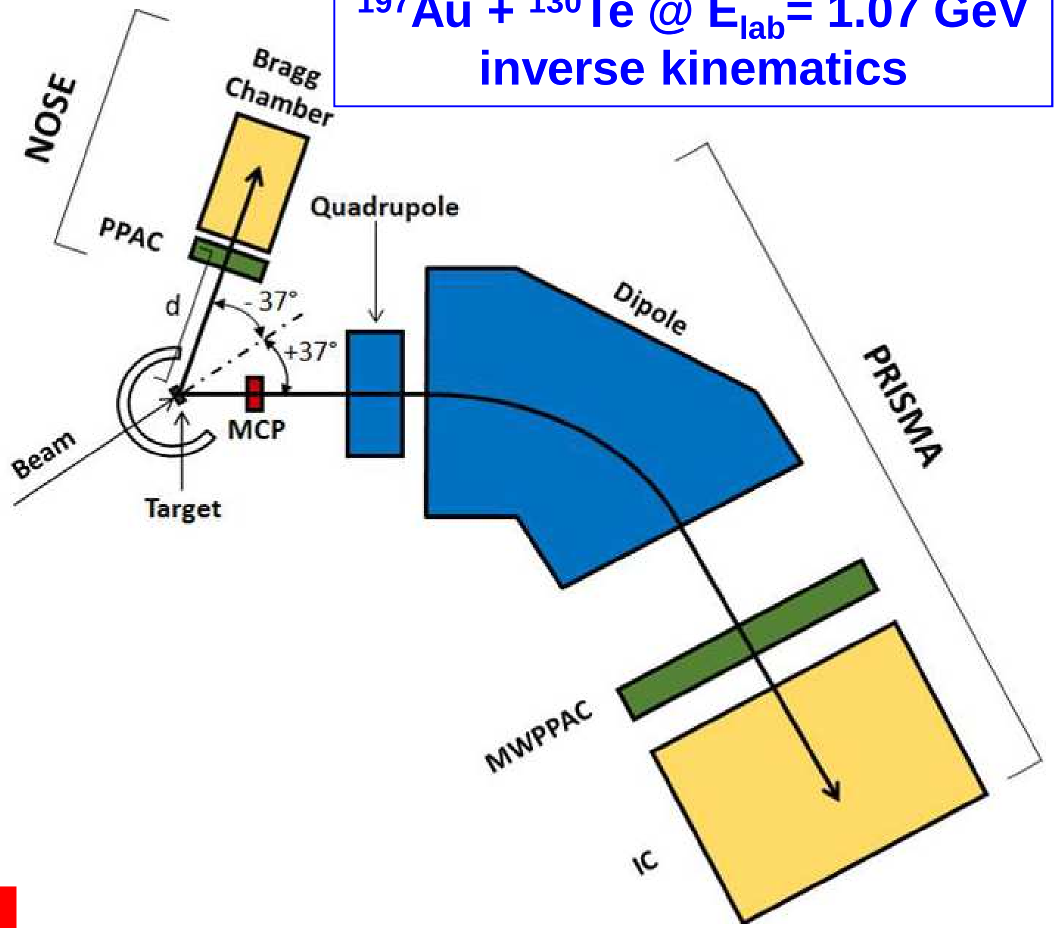

the identification in mass of the light fragment with high resolution allows to separate the mass distribution of the heavy partner in well defined bands

PRISMA spectrometer used in high resolution kinematic coincidence with a second time-of-flight system (NOSE)

F.Galtarossa et al., Phys. Rev. C97(2018)054606

The $^{136}Xe+^{238}U$ system at E_{lab} = 1 GeV AGATA+PRISMA+DANTE

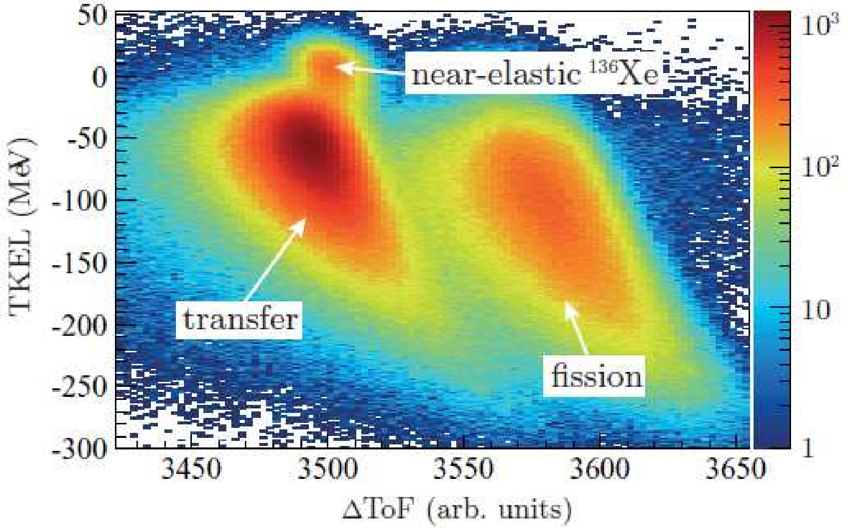

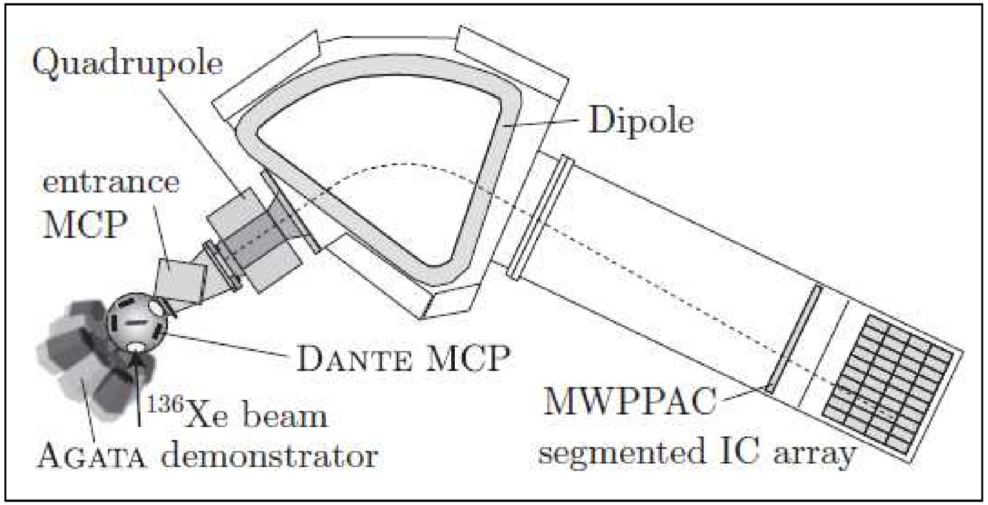

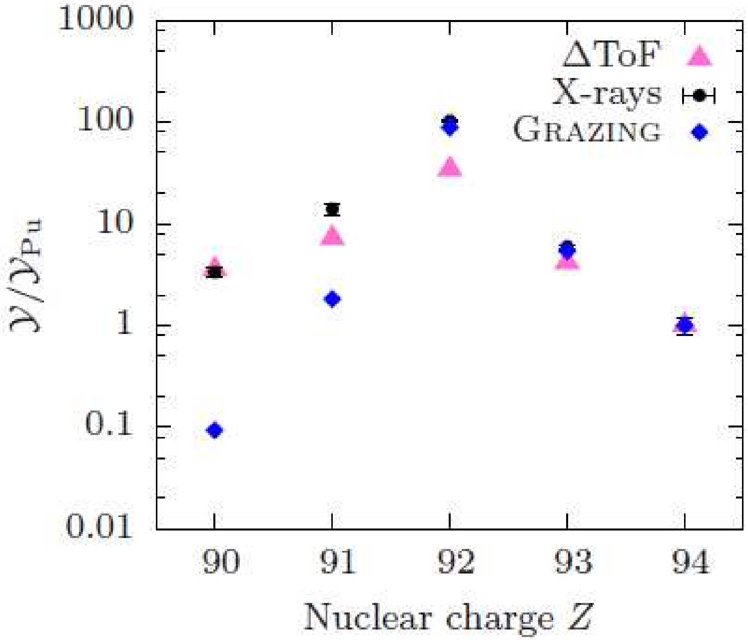

via a kinematic coincidence PRISMA-DANTE one could extract the yield of mass integrated actinide nuclei, which turns out to be in good agreement with that derived from X-ray analysis

A.Vogt et al., PRC92(2015)024619

Some take home messages

PRISMA has been so far operated in standard configuration for MNT studies

In many years of experience optimum performance has been achieved for the detection of ions with $30 < A < 130$ at 3-6 MeV/A, at angles $20^o < \theta_{lab}$ and with max 1-3 kHz trigger rate at the focal plane

For $Z < 14\text{-}16$ efficiency of MCP and MWPPAC progressively decreases

For $130\text{-}140 < A$ mass separation becomes rapidly a problem. Overlapping A/q is a yet unsolved (or unsolvable ?) issue

To get total cross sections for MNT it is generally sufficient the yield information together wih a proper normalization procedure. To get $d\sigma/d\Omega$ one needs to correct via simulations

PRISMA sensitivity limit is in the few μbarn range

Possible improvements/developments

ITEM	WHAT MIGHT BE DONE
improvement of the mass resolution, especially for A > 130-140	development of more sophisticated tracking algorithms
detection of heavy ions with higher magnetic rigidity	B increase of ~ 20% : new power supplies. Coils saturation ?
higher MWPPAC efficiency, interesting also for light masses	further developments on the new (spare) MWPPAC
improvement of the energy resolution of the IC	renewal of part of the electronics (preamplifiers and amplifiers)
improvement of the Z resolution of the IC	vertical IC position determination via electron drift time
coupling to other detectors	near the target: detectors for kinematic coincidences at the focal plane (not discussed yet)

Kinematics of the $^{206}Pb+^{118}Sn$ reaction

Calculations

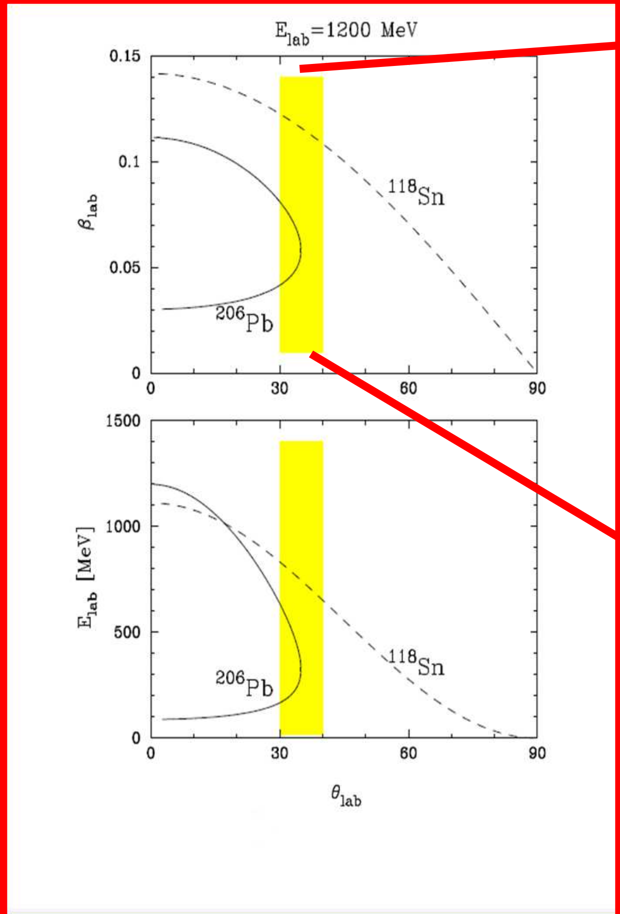

Experiment

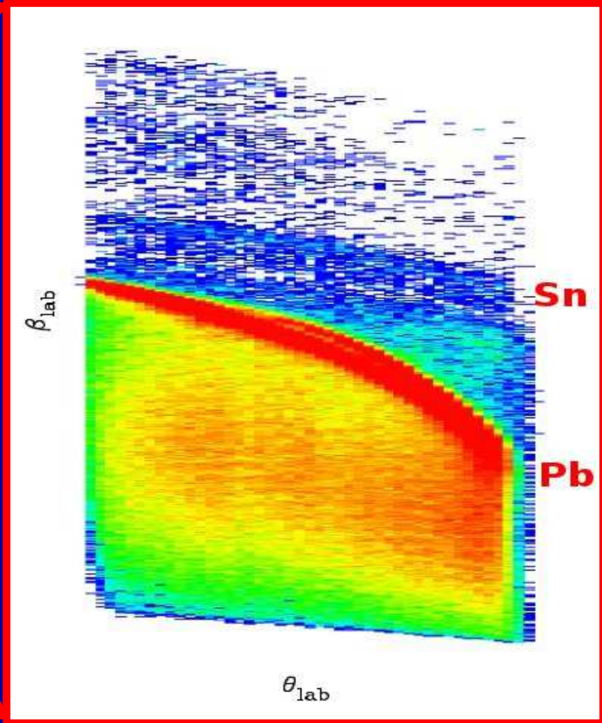

Well matched !

With PRISMA at θ_{lab}=35º Sn-like ions have kinetic energies ~ 750 MeV at E_{lab}=1200 MeV, so one expects good A,Z resolutions

θ_{lab}=35º is close to the limiting angle for Pb-like ions, so one can safely control the correct geometry of the experiment

Nuclear charge identification in the $^{206}Pb+^{118}Sn$ reaction

bombarding energy

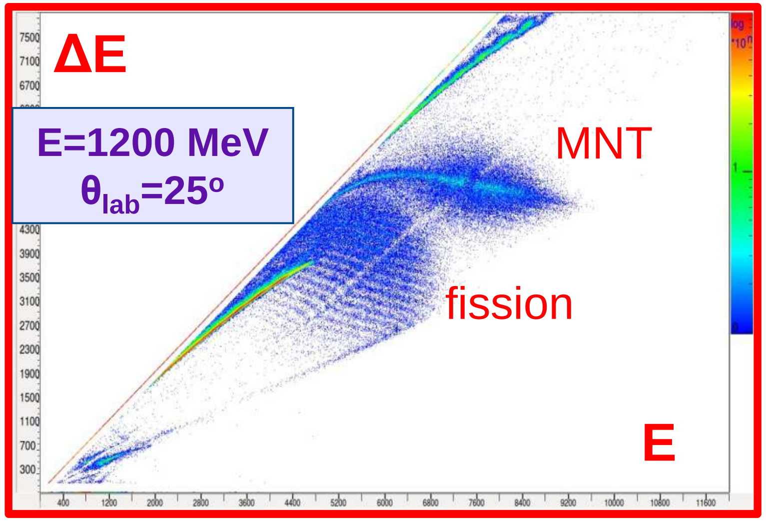

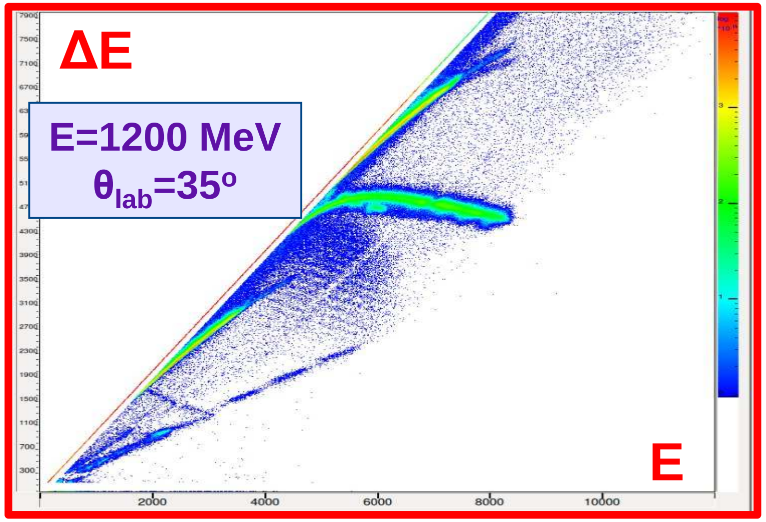

The yields of MNT (both QE ad DIC components) as well as those of fission fragments depend on both bombarding energy and angles

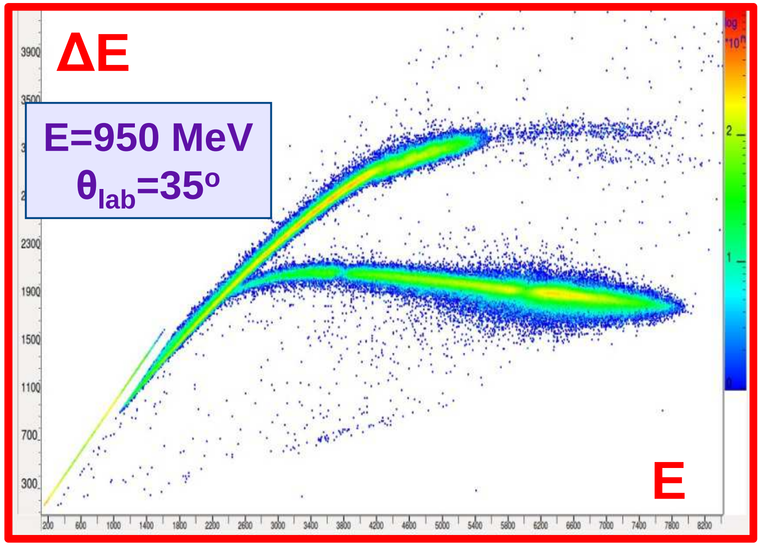

PRISMA angle

Experimental transfer probabilities

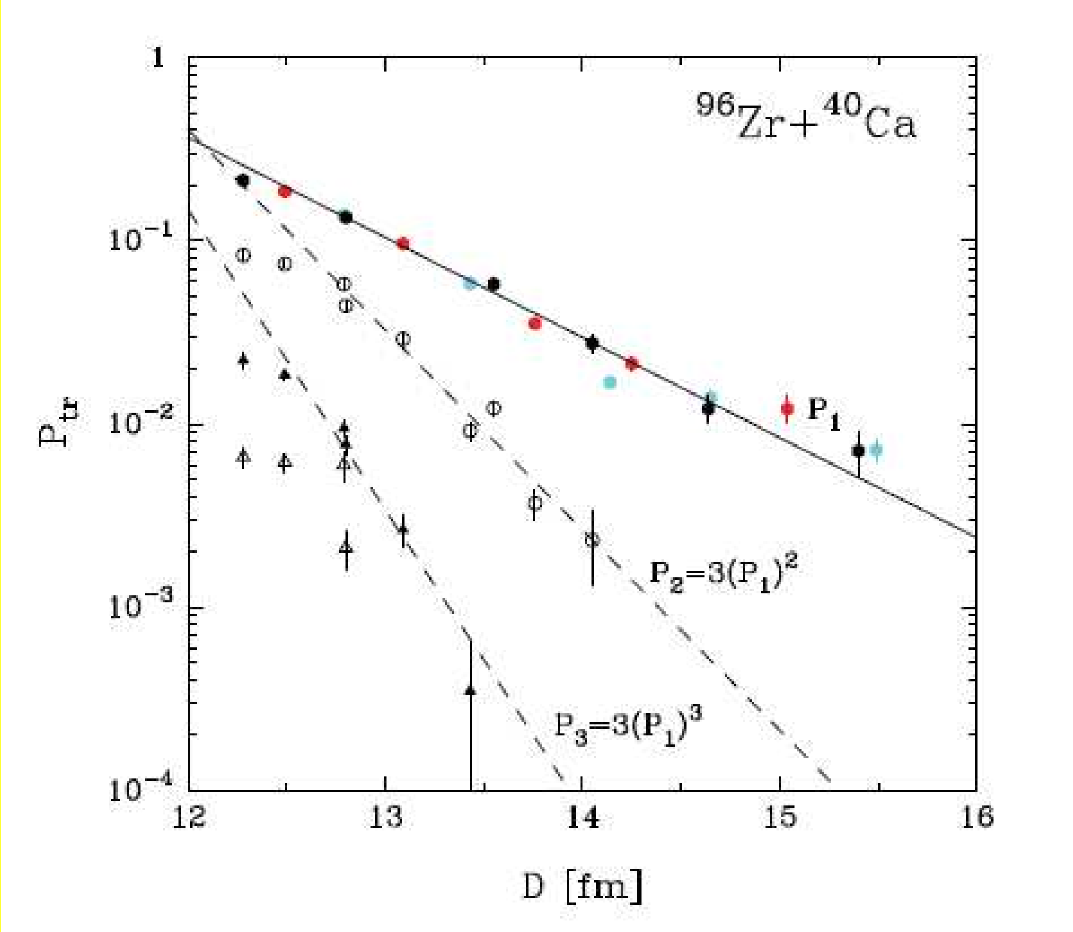

P_{tr} slope

$$P_{tr} \propto e^{-2\alpha D} \qquad \alpha = \sqrt{\frac{2mB}{\hbar^2}}$$

B → binding energy

slopes of P_{tr} vd D are as expected from the binding energies (tail of the formfactor)

a bare phenomenological analysis shows an "enhanced" pair transfer, $P_{2n} \sim 3\,(P_{1n})^2$ and $P_{3n} \sim P_{1n}(P_{2n}) \sim 3\,(P_{1n})^3$

L.Corradi et al, PRC84(2011)034603

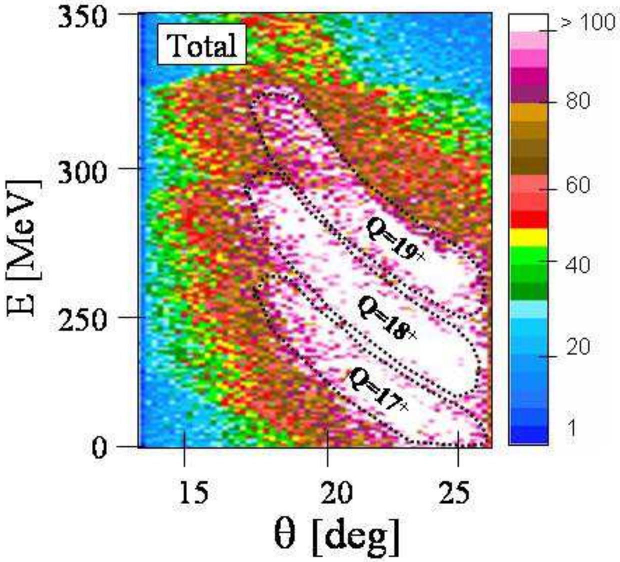

PRISMA simulations of ion transport

Correction factors derived from bidimensional E-θ uniform input distributions

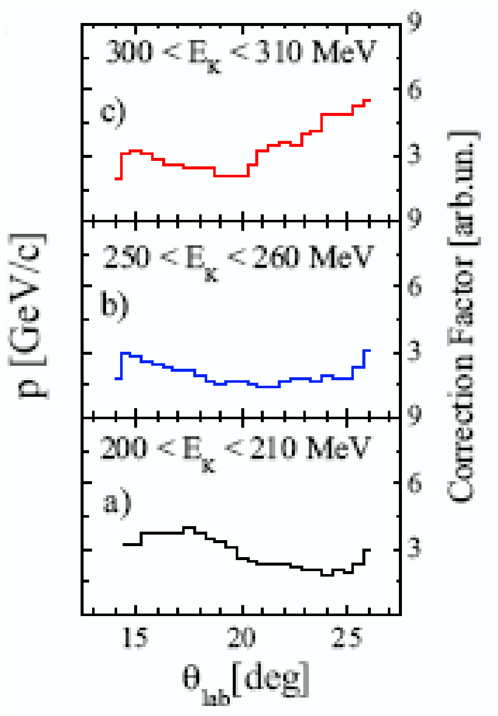

$^{48}Ca+^{64}Ni$ E=270 MeV

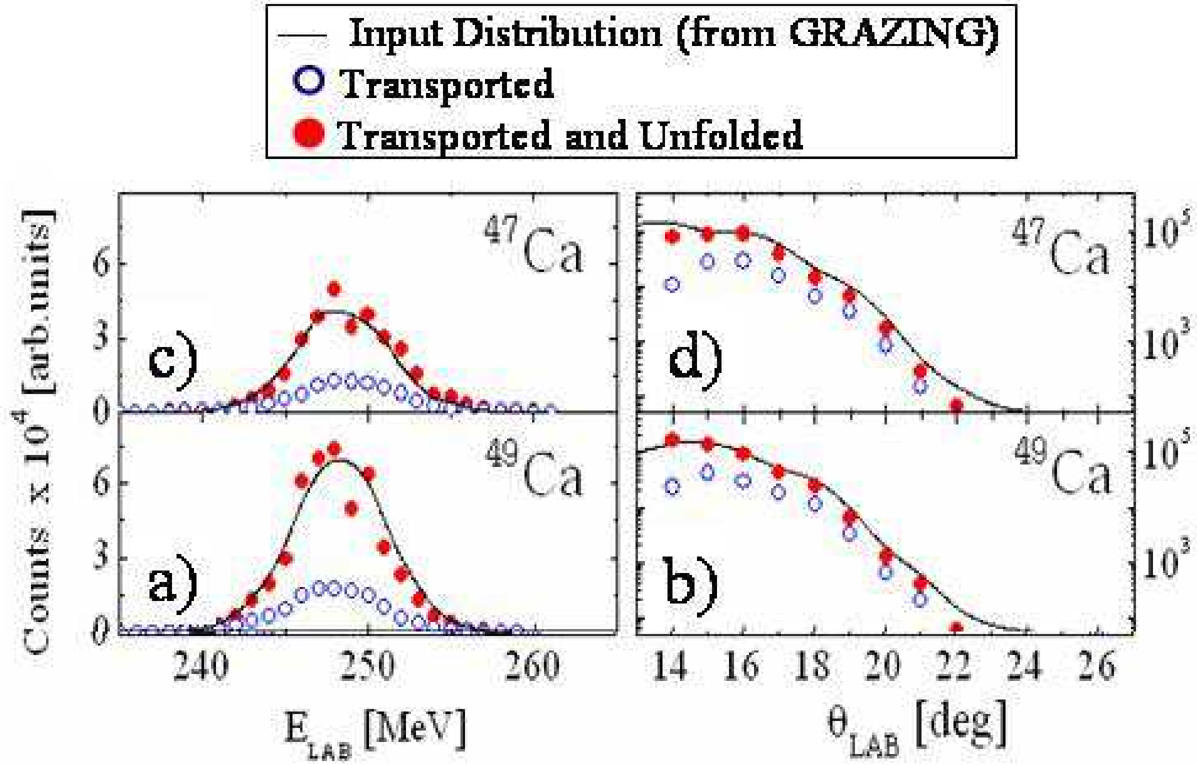

D.Montanari et al, EPJ A47(2011)4

Cross section measurements in $^{82}Se+^{238}U$ at E_{lab}=505 MeV

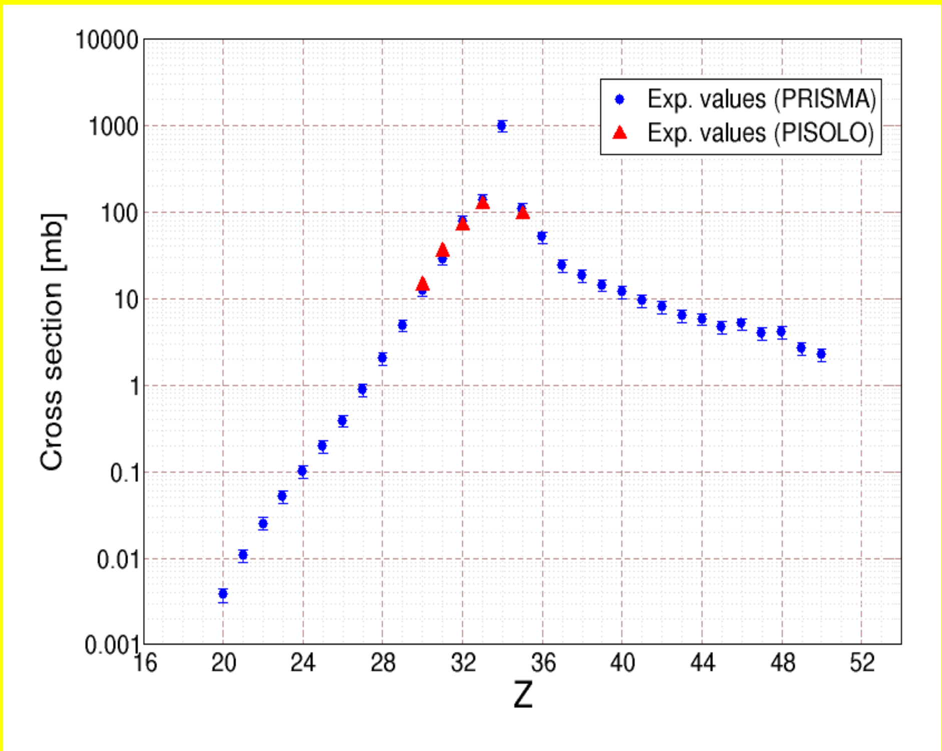

Cross sections for exotic nuclei like the N=50 ^{82}Ge or ^{80}Zn could be mesaured down to few μb level

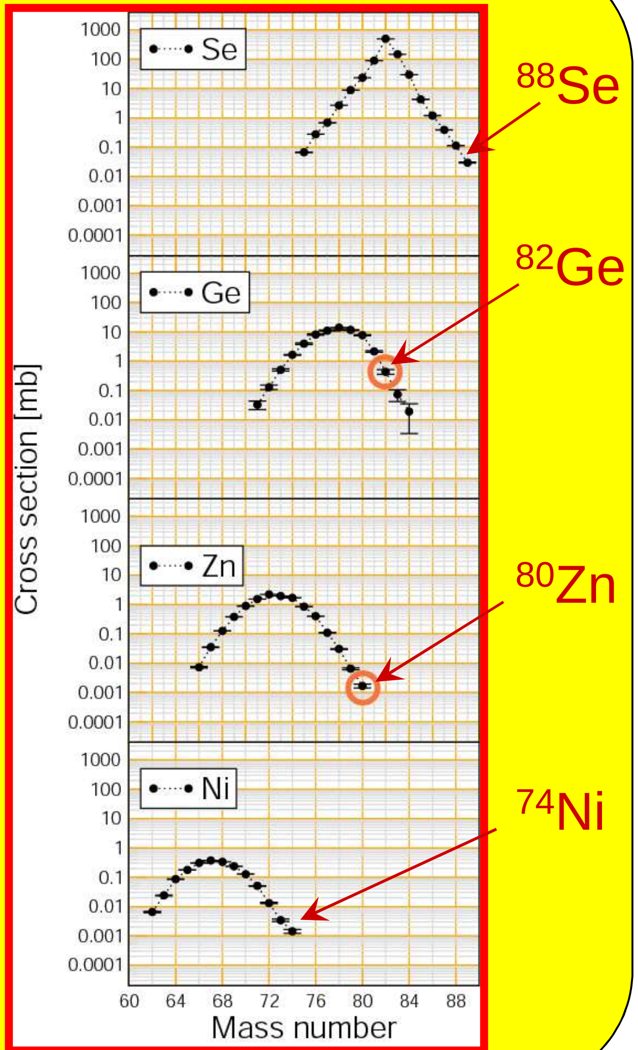

The ^{197}Au+^{130}Te experiment with the PRISMA spectrometer

^{197}Au + ^{130}Te @ E_{lab}= 1.07 GeV
inverse kinematics

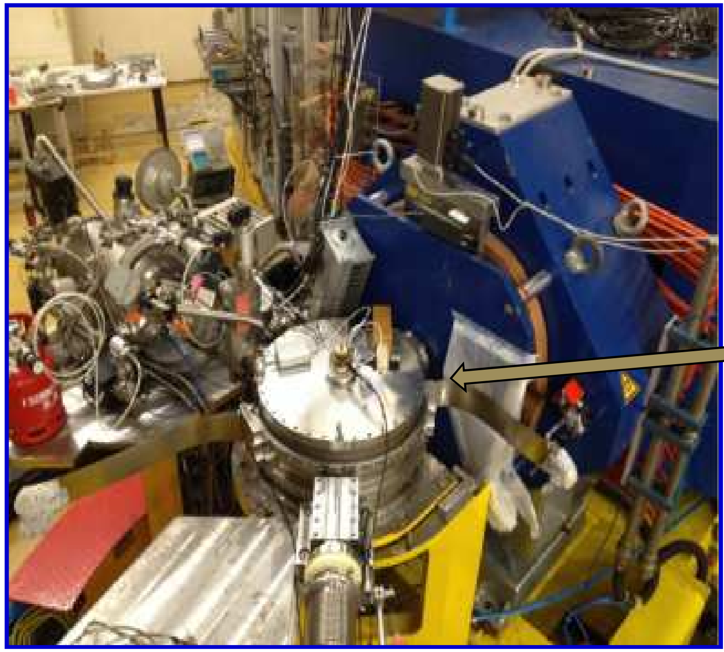

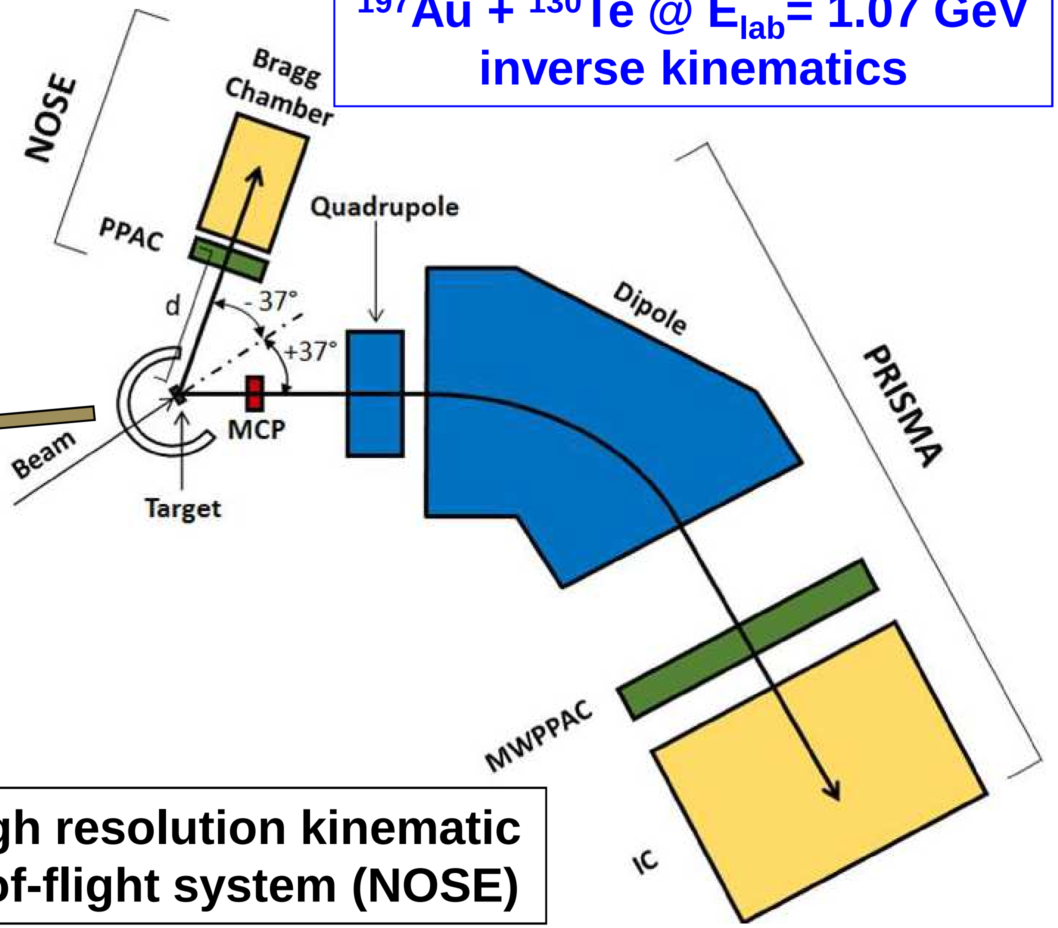

PRISMA spectrometer used in high resolution kinematic coincidence with a second time-of-flight system (NOSE)

PRISMA ⟶ A,Z of light Te-recoils - ΔA/A ~ 1/240

NOSE ⟶ A,Z of heavy Au-projectiles - ΔA/A ~ 1/40

F.Galtarossa et al., Phys. Rev. C97(2018)054606

$^{197}Au+^{130}Te$: mass-mass correlation matrix

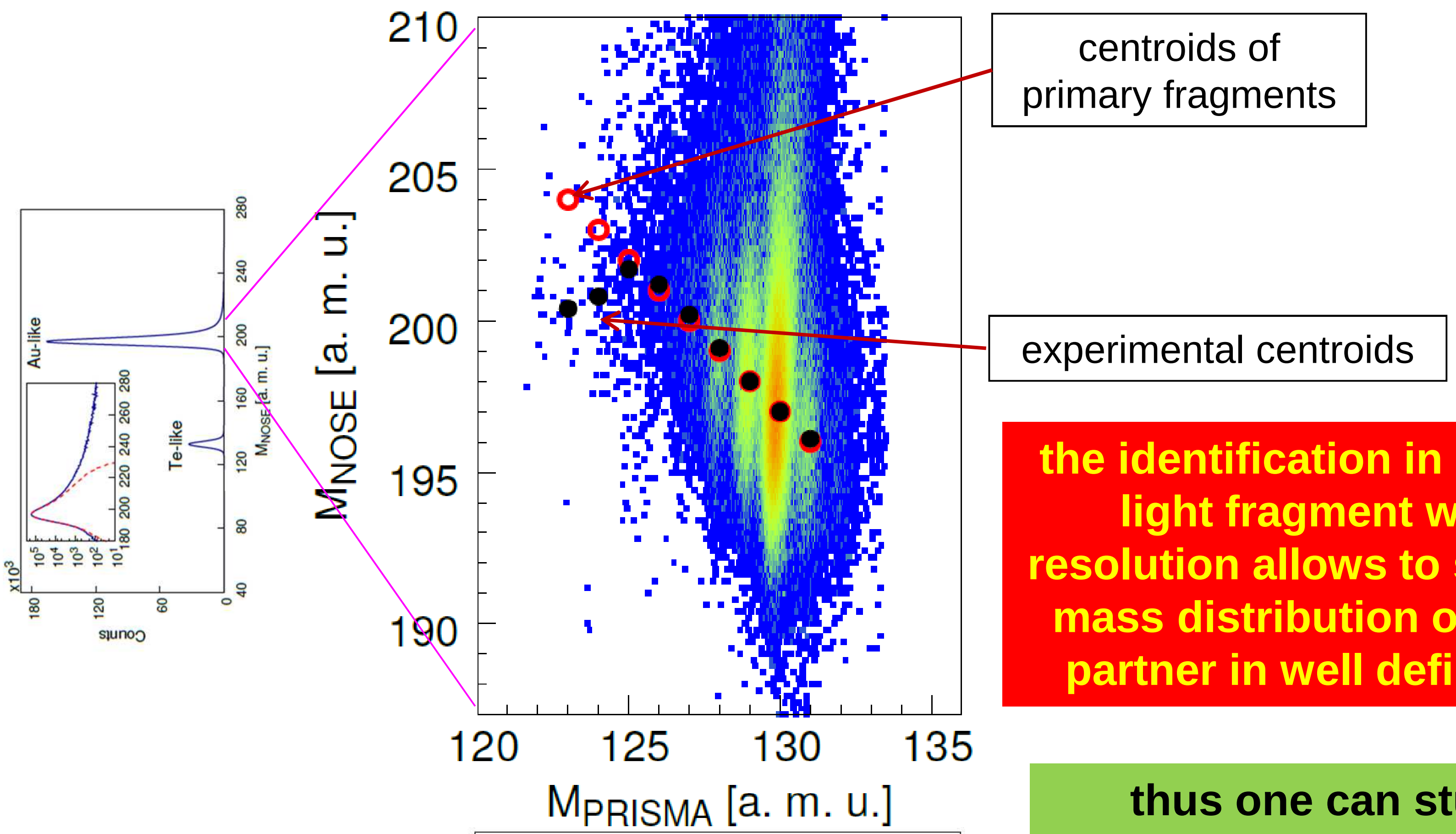

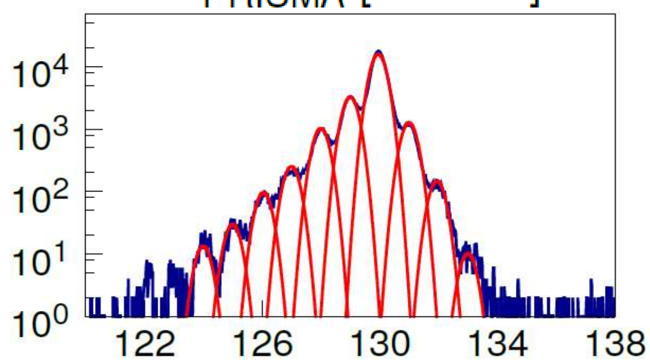

the identification in mass of the light fragment with high resolution allows to separate the mass distribution of the heavy partner in well defined bands

thus one can study the evolution of the mass centroids and widths of the heavy partners, which are correlated to the effect of secondary processes

Change of population pattern from neutron-poor to neutron-rich projectiles

LNL data

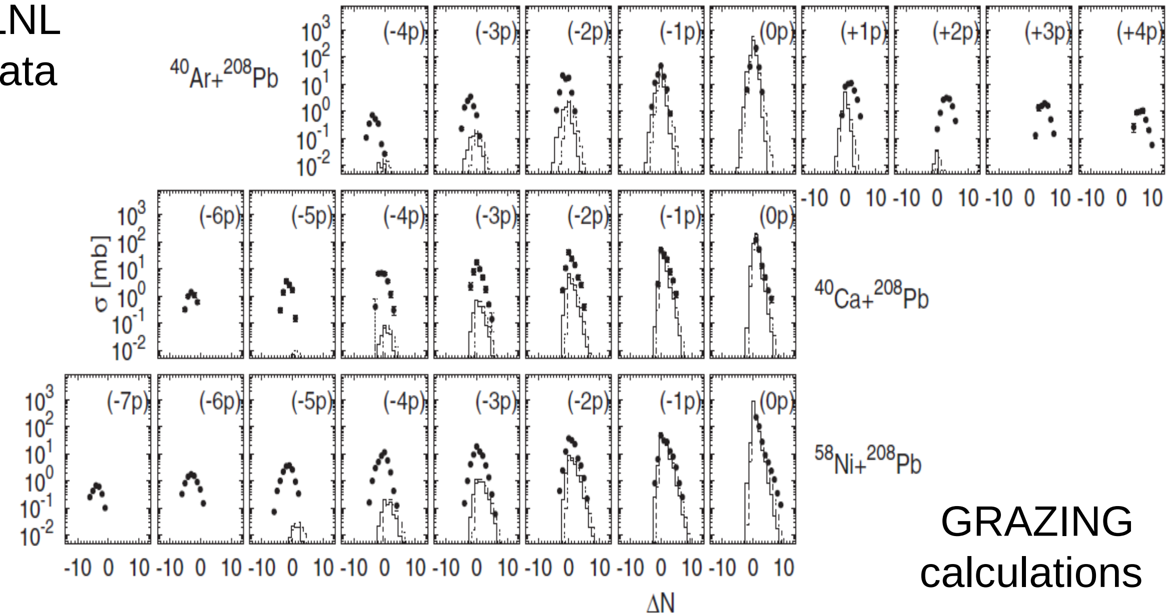

GRAZING calculations

at above barrier many open transfer channels become available

for large TKEL secondary processes play a major role in the final mass distribution

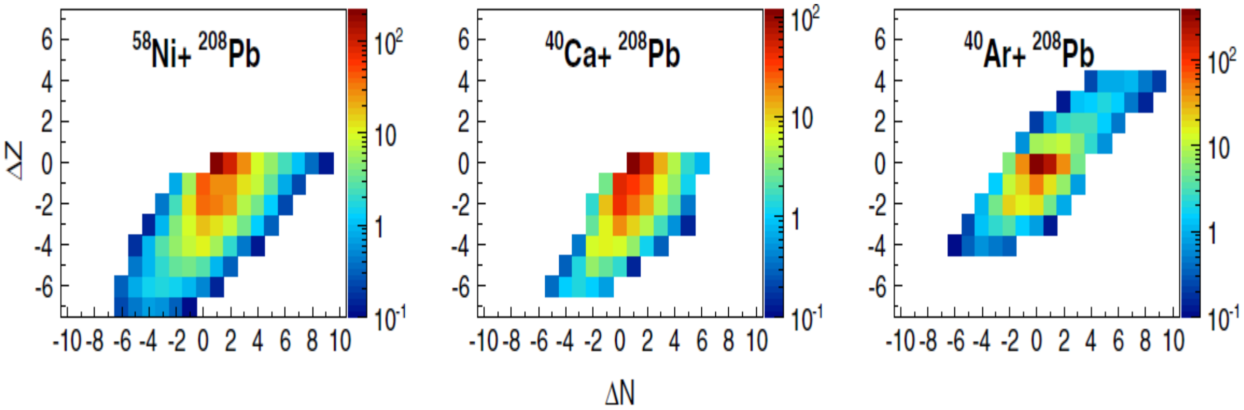

Wilczynski plots

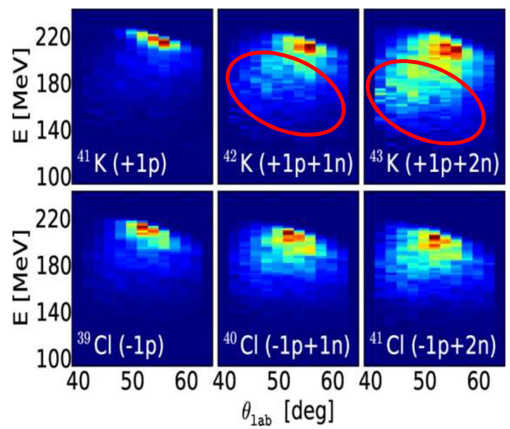

^{40}Ar+^{208}Pb

T. Mijatovic et al., Phys. Rev. C 94 (2016) 064616

Evaporation processes in multinucleon transfer reactions

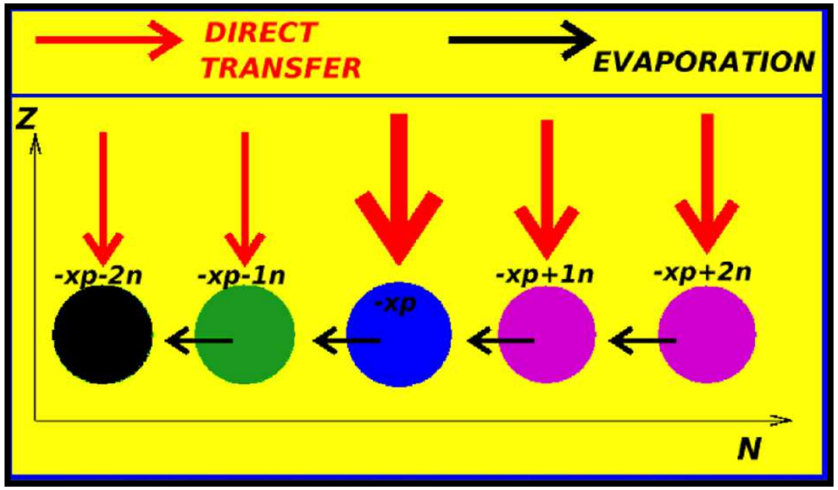

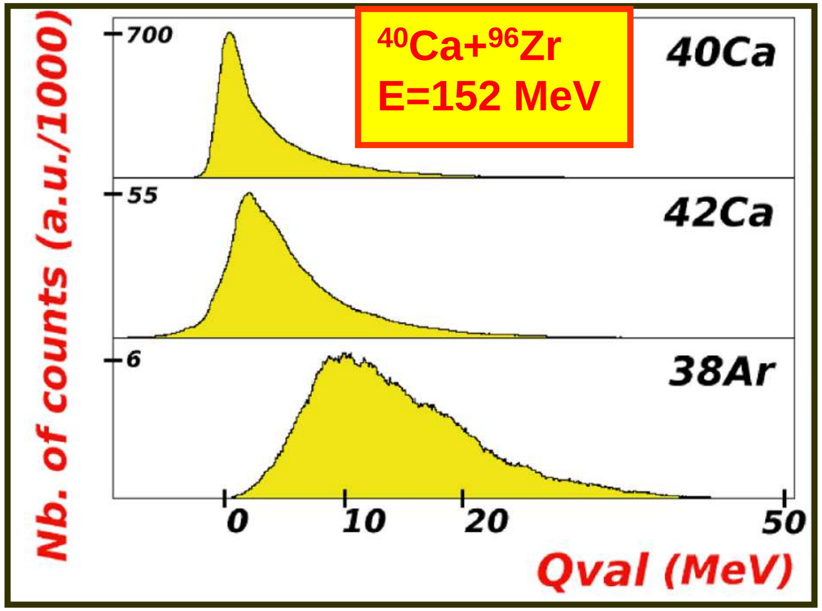

Direct identification with PRISMA+CLARA

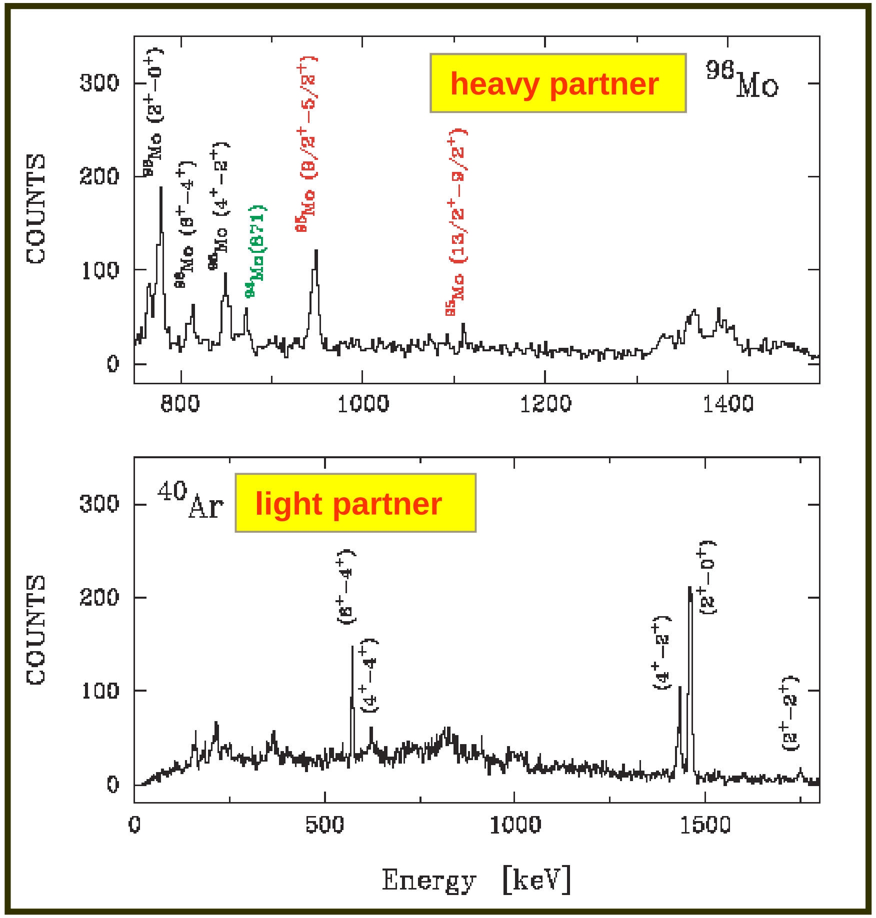

Population of neutron rich nuclei via multinucleon transfer

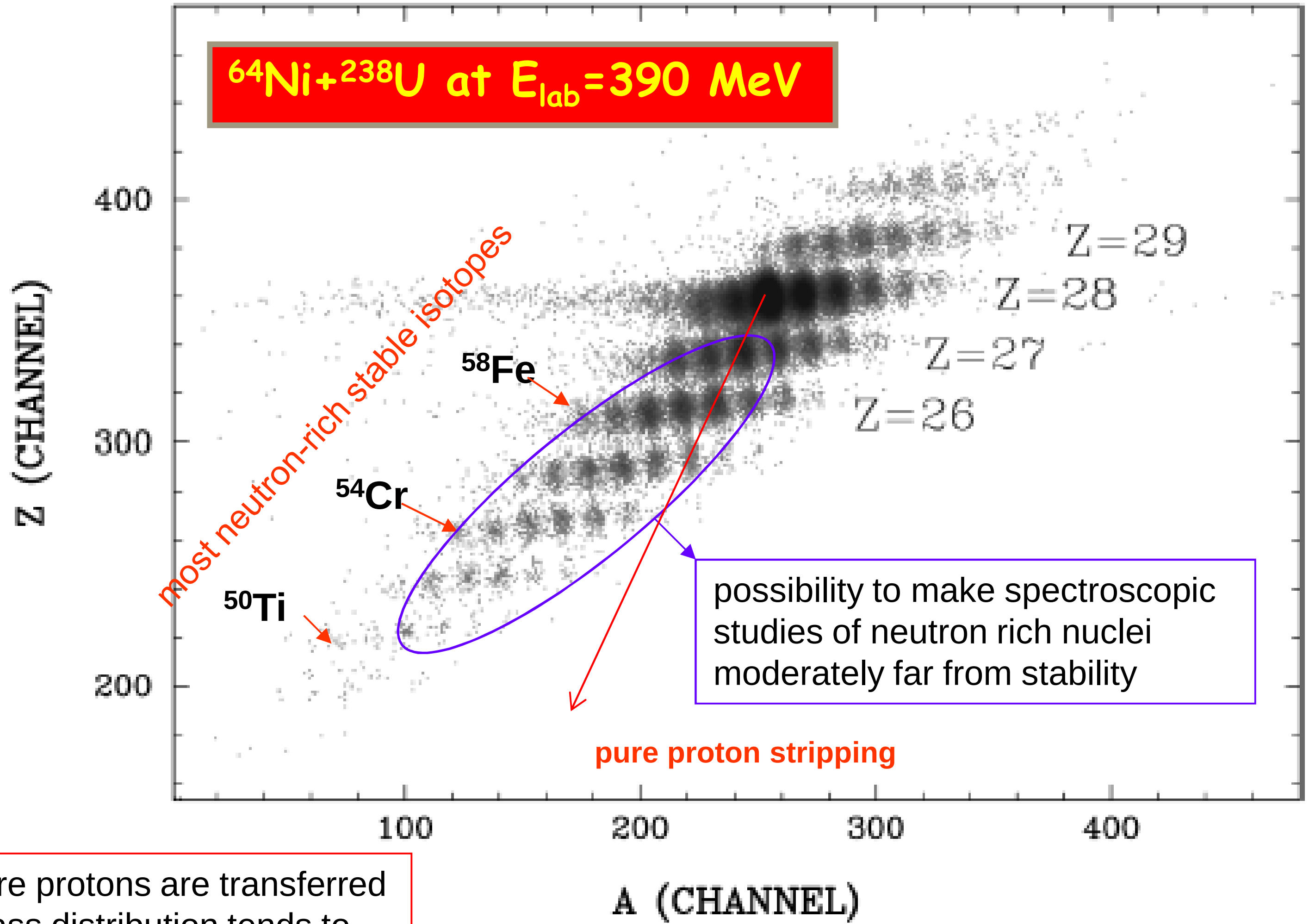

as more protons are transferred the mass distribution tends to shift to lower values due to neutron evaporation

L.Corradi et al, Phys.Rev.C59(1999)261

Pair neutron transfer probed via γ-particle coincidence

by using the strength obtained with the gamma data for the inelastic and neutron transfer channels and with information from coupled-channel calculations we were able to quote that the fraction of the 2n channel populating the ground to ground state is larger than 76 %

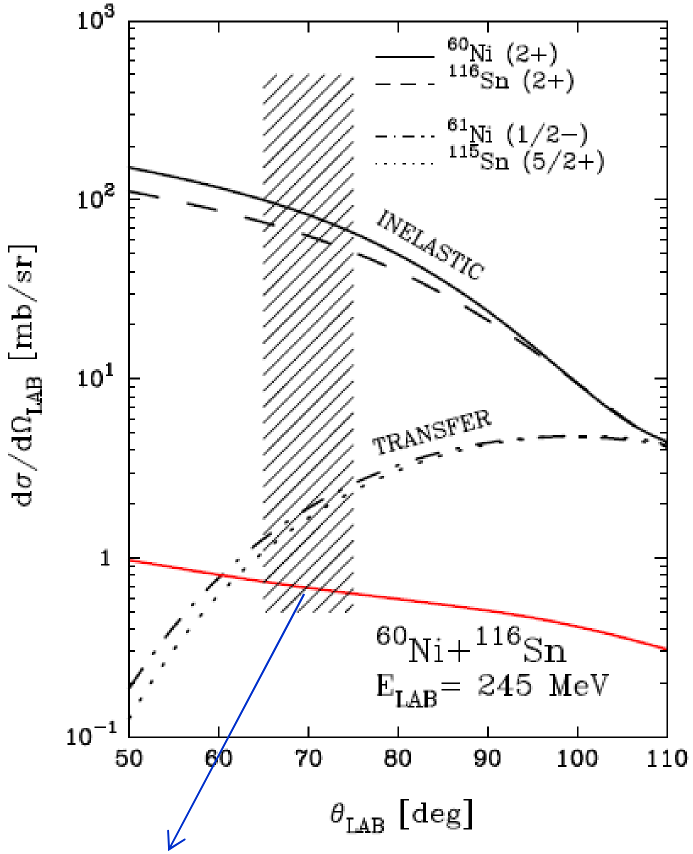

$$\sigma_R\left(1-\frac{\sigma_{el}}{\sigma_R}\right)=\sigma(2^+,{}^{60}\mathrm{Ni})\left(1+\frac{\sigma(2^+,{}^{116}\mathrm{Sn})}{\sigma(2^+,{}^{60}\mathrm{Ni})}\right)$$

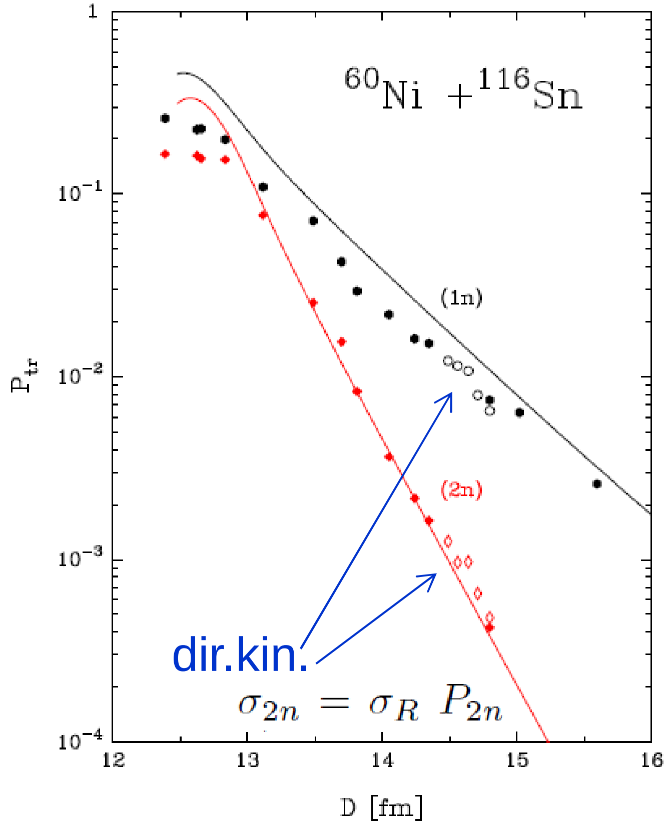

consistent comparison between inverse kinematics and direct kinematics data

$^{197}Au+^{130}Te$: cross sections for the Te isotopes

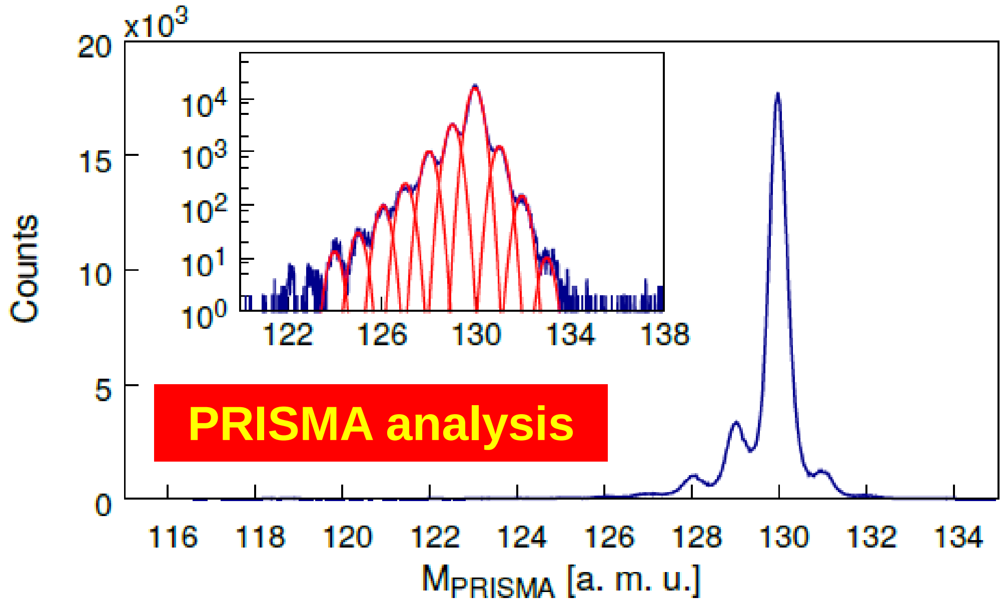

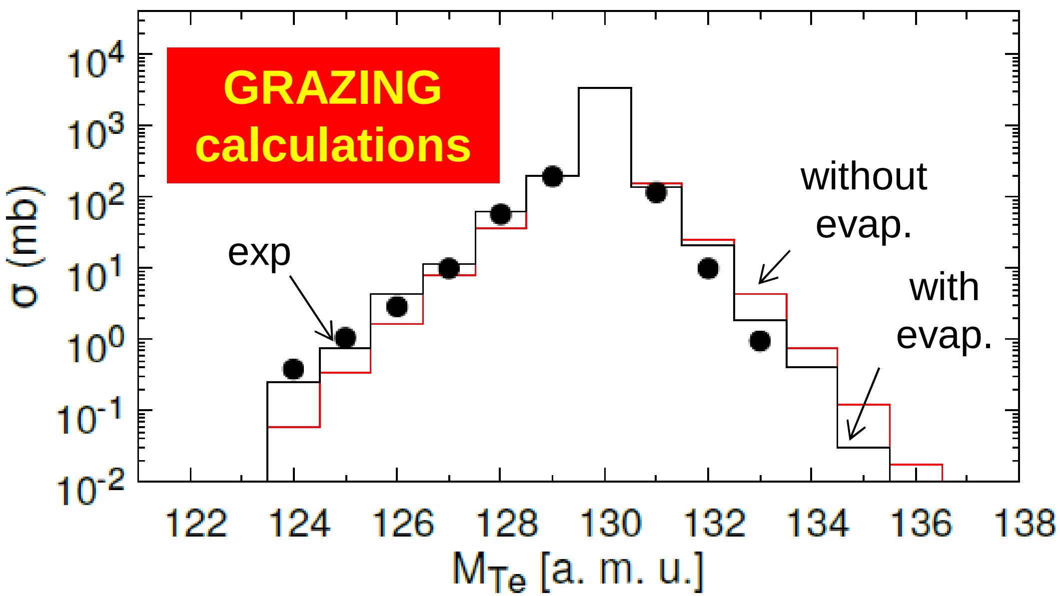

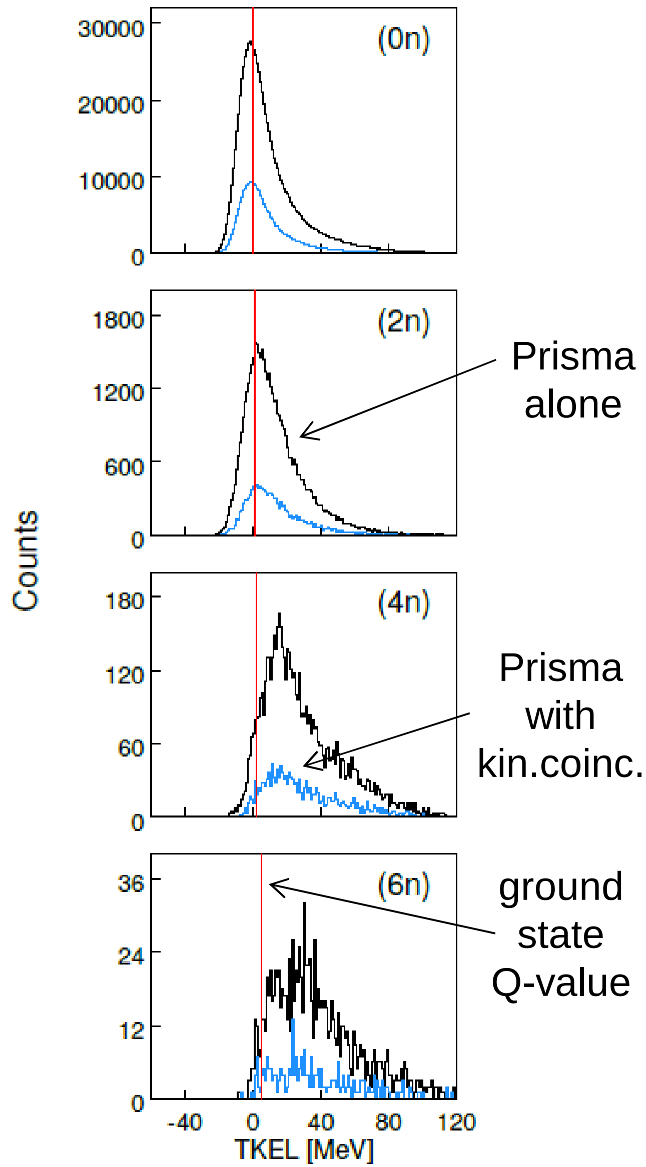

F. Galtarossa et al.

^{197}Au+^{130}Te : mass-mass correlation, experiment and Monte Carlo simulations

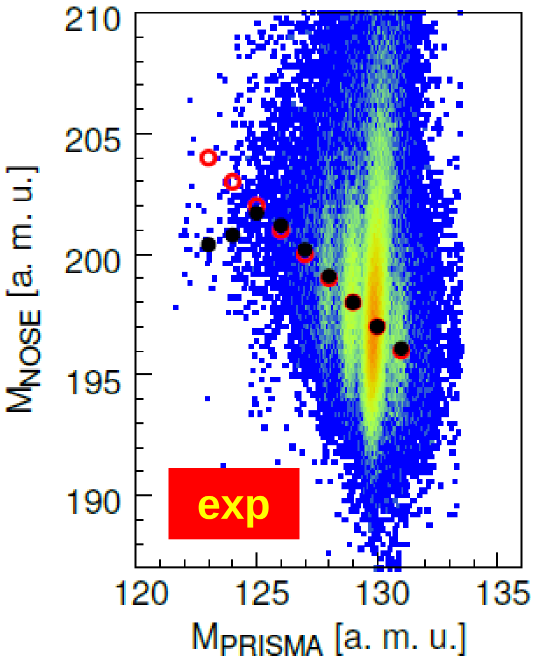

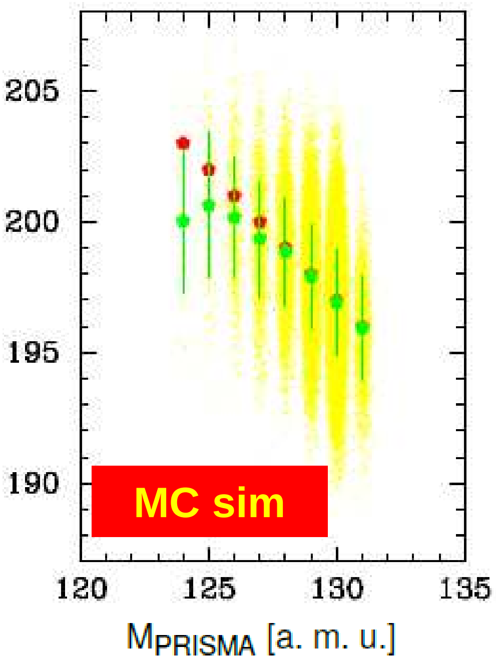

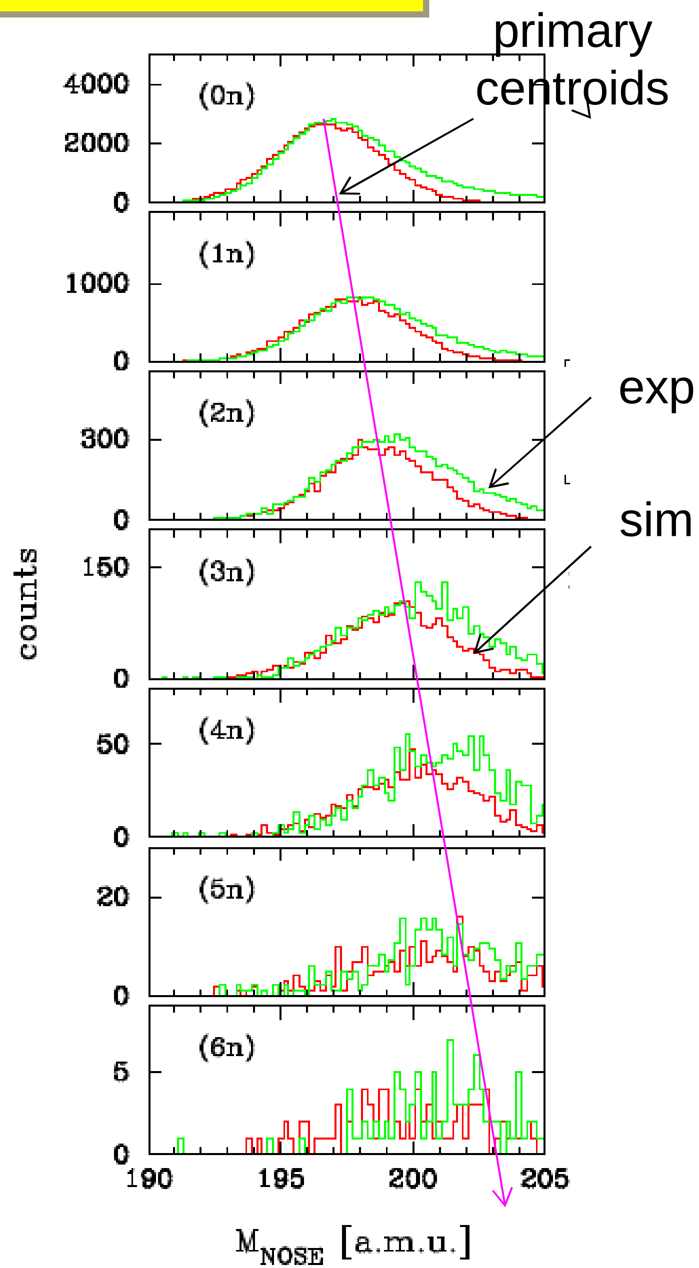

simulations incorporate the full kinematics and take into account the TKEL distributions (to compute evaporation) and σ measured in Prisma

the simulations indicate that the shift of the centroids towards lower masses and the width enlargment is due to evaporation

Multianode ionization chamber : Z discrimination for different ions

ΔE/E < 2%

Z/ΔZ ~ 60 for Z=20

^{40}Ar+^{208}Pb 450 MeV

^{70}Zn+^{238}U 450 MeV

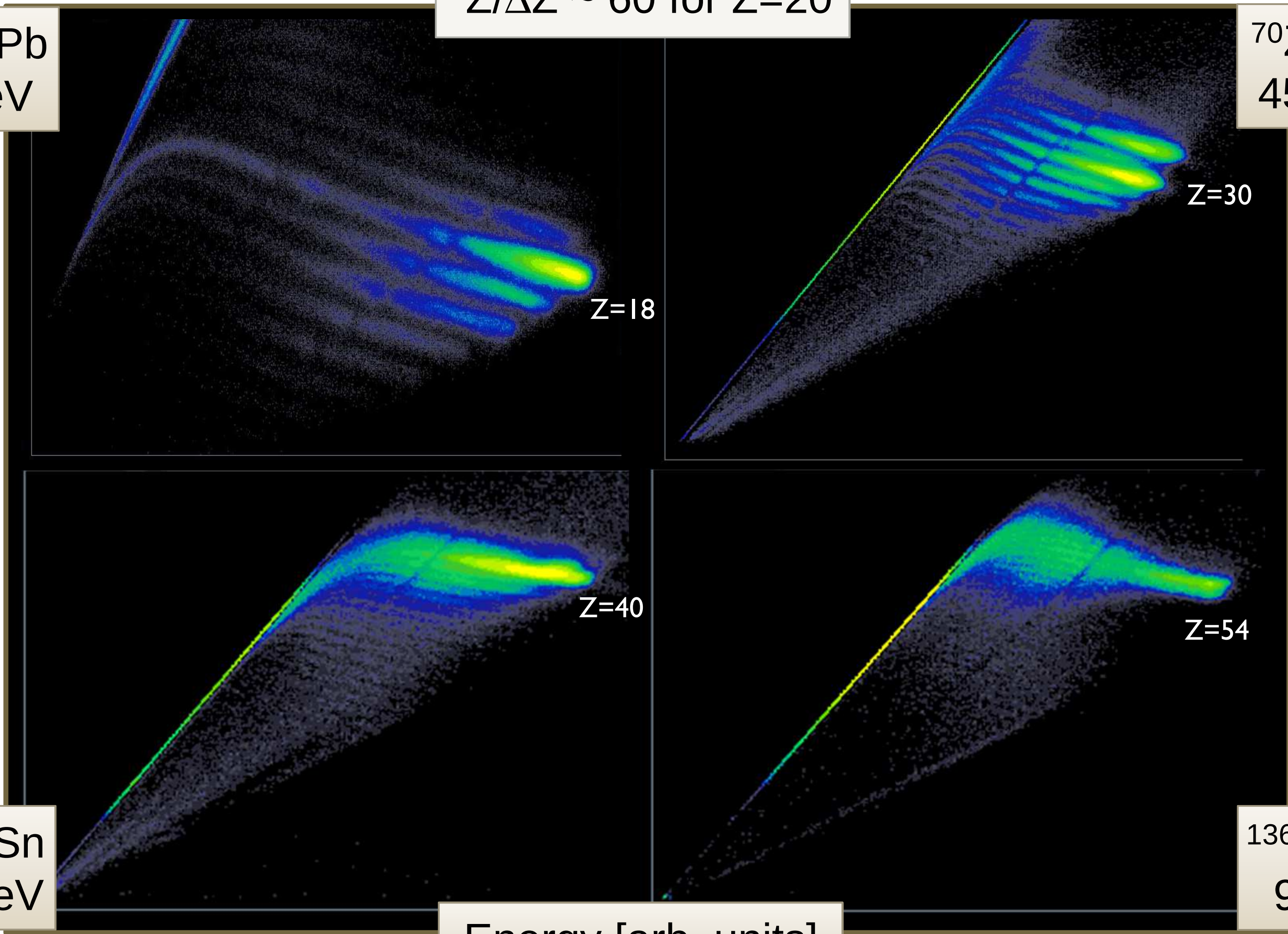

^{96}Zr+^{124}Sn 575 MeV

^{136}Xe+^{208}Pb 950 MeV

Energy [arb. units]

Multianode ionization chamber : optimization for Z discrimination

$^{96}Zr+^{124}Sn$ @ E_{lab}=500 MeV

ΔE (1^{st} stage) [arb. units]

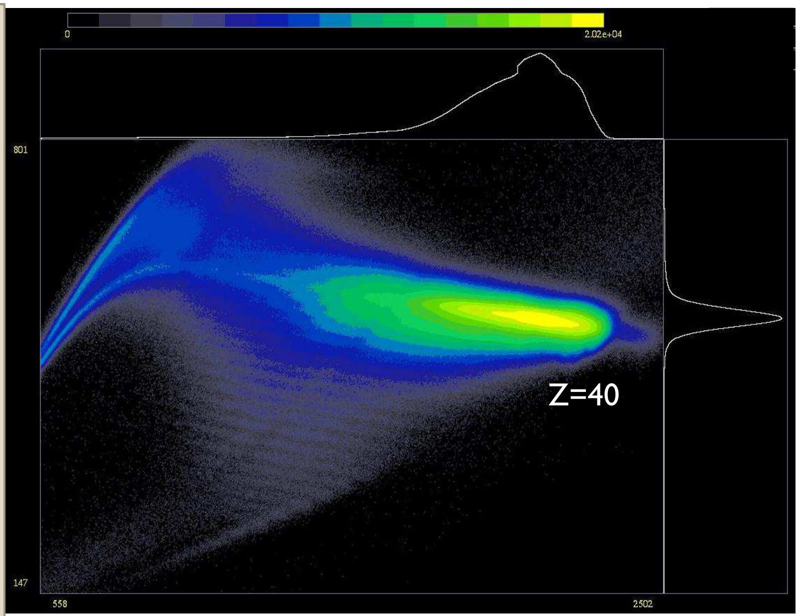

Energy [arb. units]

ΔE ($1^{st}+2^{nd}$ stages) [arb. units]

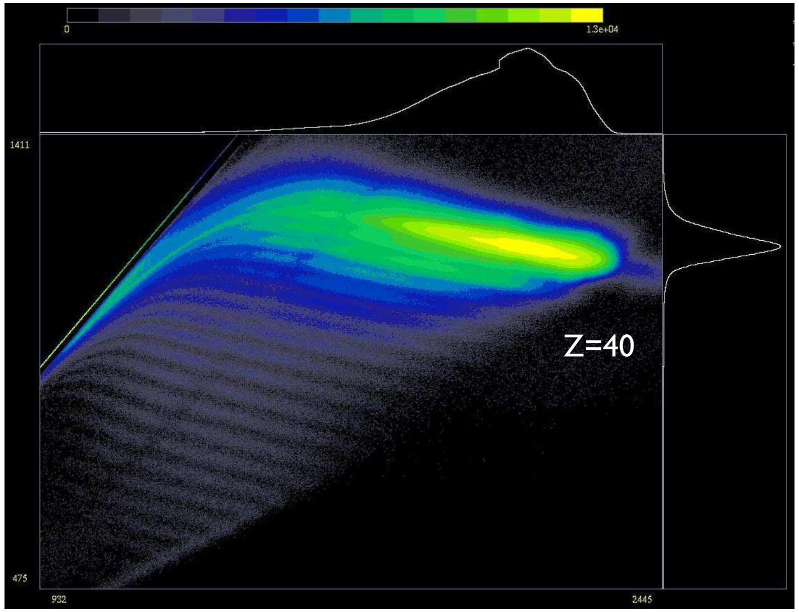

Energy [arb. units]

Optimal ΔE thickness

IC Working pressure

Number of IC sections per ΔE

Neutron rich nuclei produced in the fission of ^{238}U in $^{136}Xe + ^{238}U$ at E_{lab}=990 MeV

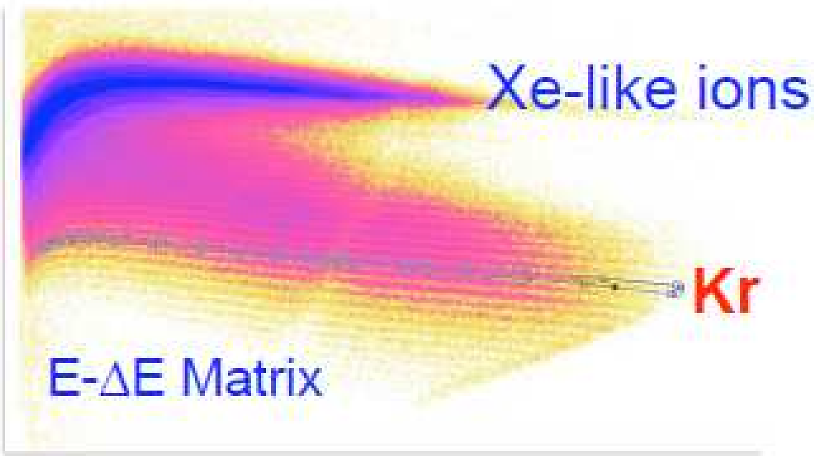

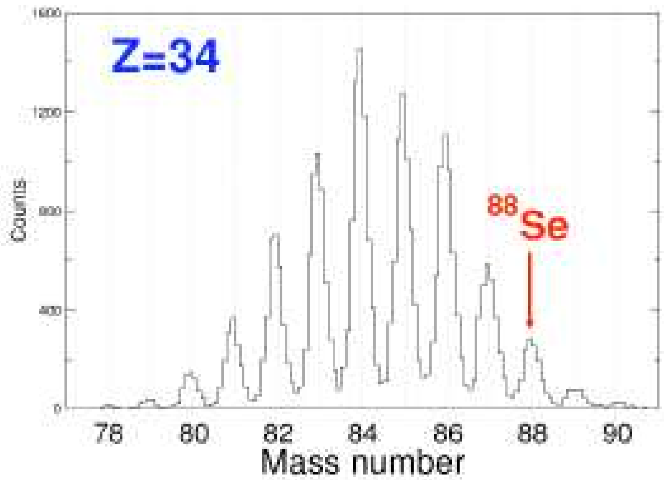

Cross sections for mass integrated Z distributions

LNL 2007

$^{82}Se+^{238}U$ E_{lab}=505 MeV

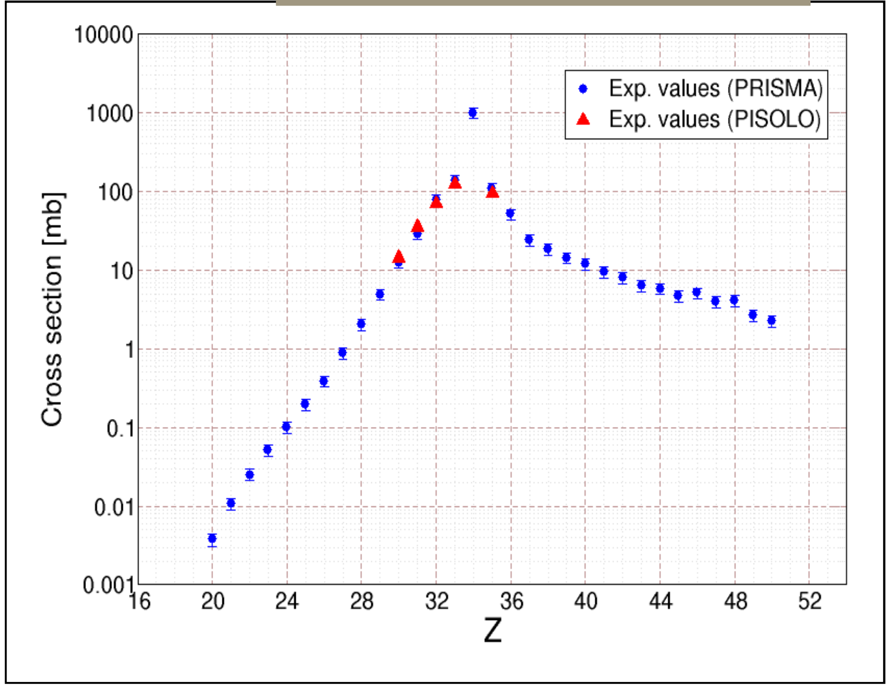

total yields obtained with PRISMA well overlap with values previously measured with the time-of-flight spectrometer PISOLO

GSI 1977

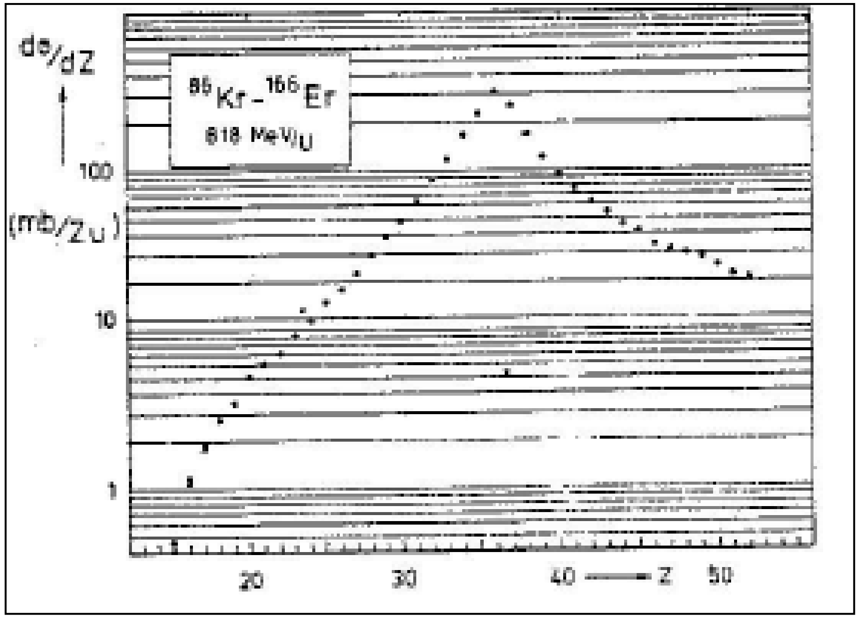

while the trend on the left side of the Z of the projectile is dominated by transfer processes, the one on the right side is affected by fission